Available online at www.sciencedirect.com
SCIENCE DIRECT®
Journal of Computational Physics 187 (2003) 391–427
JOURNAL OF COMPUTATIONAL PHYSICS
www.elsevier.com/locate/jcp

Finite volume schemes with equilibrium type discretization of source terms for scalar conservation laws

Ramaz Botchorishvili [a,b], Olivier Pironneau [b,*]

[a] VIAM, Tbilisi State University, 2 University Street, Tbilisi 380043, Georgia
[b] Laboratoire d'Analyse Numérique, Université Pierre et Marie Curie, France

Received 27 June 2002; received in revised form 7 December 2002; accepted 30 January 2003

Abstract

We develop here a new class of finite volume schemes on unstructured meshes for scalar conservation laws with stiff source terms. The schemes are of equilibrium type, hence with uniform bounds on approximate solutions, valid in cell entropy inequalities and exact for some equilibrium states. Convergence is investigated in the framework of kinetic schemes. Numerical tests show high computational efficiency and a significant advantage over standard cell centered discretization of source terms. Equilibrium type schemes produce accurate results even on test problems for which the standard approach fails. For some numerical tests they exhibit exponential type convergence rate. In two of our numerical tests an equilibrium type scheme with 441 nodes on a triangular mesh is more accurate than a standard scheme with 5000^2 grid points.

AMS: 65M06; 65M12

Keywords: Hyperbolic conservation laws; Finite volume schemes; Stiff source terms; Convergence

1. Introduction

Consider the following multidimensional scalar conservation law with source term:

$$\frac{\partial u}{\partial t}+\sum_{i=1}^{N}\frac{\partial A_i(u)}{\partial x_i}+b(u)\sum_{i=1}^{N}\frac{\partial z_i(x)}{\partial x_i}=0,\quad t\geqslant 0,\ x\in\mathbb{R}^N, \tag{1.1}$$

$$u(0,x)=u_0(x),\quad u_0(x)\in L^1\cap L^\infty, \tag{1.2}$$

* Corresponding author. Present address: University of Paris VI, Analyse Numerique, 175 Rue du Chevaleret, Paris F-75013, France.
E-mail address: pironneau@ann.jussieu.fr (O. Pironneau).
URL: http://www.ann.jussieu.fr/pironneau.

0021-9991/03/$ - see front matter
doi:10.1016/S0021-9991(03)00086-X

with smooth functions $A_i(\cdot)$, $z_i(x)$, $b(\cdot)$, $A_i \in C^1(\mathbb{R})$, $z_i(x) \in C^1(\mathbb{R}^N)$, $1 \leqslant i \leqslant N$, $b \in C^1(\mathbb{R})$,

$$|\nabla \vec{z}(x)| \leqslant K_z, \quad K_z = cst, \quad b(0) = 0, \quad \|b'\|_{L^\infty} \leqslant K_b, \quad K_b = cst, \tag{1.3}$$

where the unknown function $u(t,x)$ belongs to $\mathbb{R}$. Eq. (1.1) is endowed with the full family of entropy inequalities

$$\frac{\partial S(u)}{\partial t} + \sum_{i=1}^{N} \frac{\partial \eta_i(u)}{\partial x_i} + S'(u)b(u) \sum_{i=1}^{N} \frac{\partial z_i(x)}{\partial x_i} \leqslant 0, \tag{1.4}$$

for all convex entropy functions $S(\cdot)$ and corresponding entropy fluxes $\eta_i(\cdot)$ that are defined in accordance with the relation

$$\eta_i'(u) = S'(u)a_i(u), \quad a_i(u) = A_i'(u), \tag{1.5}$$

see Kruzkov [27], Lax [30] for more details.

A numerical difficulty which arises in connection with problem (1.1), (1.2) is to preserve, at a discrete level, the "equilibrium", i.e., steady states given by

$$\sum_{i=1}^{N} \frac{\partial}{\partial x_i}(D_i(u) + z_i(x)) = 0, \tag{1.6}$$

where

$$D_i(u) = \int_0^u \frac{a_i(s)}{b(s)}\,\mathrm{d}s < +\infty, \quad 1 \leqslant i \leqslant N. \tag{1.7}$$

In [7] the class of *equilibrium schemes* have been introduced, i.e., solvers ensuring that

equilibrium initial data are maintained, (1.8)

all the discrete entropy inequalities are valid, (1.9)

approximate solutions are, locally in time L^∞ *bounded*. (1.10)

For scalar conservation laws in one dimension the convergence of equilibrium schemes has been proved and their computational efficiency has been demonstrated [7].

In single space dimension, i.e., when $N = 1$, integration of Eq. (1.6) results in simple two point formulae that enables to define discrete equilibria and to control (1.8). In several space dimensions integration of (1.6) over some open domain Ω yields:

$$\int_{\partial\Omega} \langle D(u) + z(\gamma), \vec{n}(\gamma)\rangle\,\mathrm{d}\gamma = 0, \tag{1.11}$$

where $\langle\cdot,\cdot\rangle$ denotes scalar product in $\mathbb{R}^N$, $\gamma \in \partial\Omega$, $\vec{n} = (n_1, \ldots, n_N)$ is unit normal vector of the boundary $\partial\Omega$. Even if we know u in some points on $\partial\Omega$ there is no way to compute the integral in left-hand side of (1.11) exactly. Thus in multidimension it is difficult to define and make explicit the discrete equilibrium states. That is why in [8] the requirement (1.8) has been modified and replaced by less general requirement on maintenance of some specific equilibria. Here we reformulate the requirement from [8] in terms of locally one dimensional equilibria.

Definition 1. $u(x)$ has a locally one dimensional equilibrium in direction $\vec{n}$ in points x_j and x_k if

$$\langle D(u(x_j)) + z(x_j), \vec{n}\rangle = \langle D(u(x_k)) + z(x_k), \vec{n}\rangle. \tag{1.12}$$

The following lemma gives sufficient condition for locally one dimensional equilibrium states.

Lemma 1.0.1. *Solution of* (1.6) $u(x)$ *has a locally one dimensional equilibrium in direction* $\vec{n}$ *in points* x_j *and* x_k *if there exist open connected domain* Ω *such that*

1. $x_j, x_k \in \Omega$,

2. $\langle D(u(x)) + z(x), \vec{n}\rangle \in C(\{P_{N-1}(x_j, \vec{n}) \cup P_{N-1}(x_j, \vec{n})\} \cap \Omega)$,

3. $\langle D(u(y)) + z(y), \vec{\tau}_k(x)\rangle = c_x(y), \quad c_x(y) = cst, \;\; y \in P_{N-1}(x, \vec{n}) \cap \Omega, \;\; x \in \Omega \setminus \{x_j\} \setminus \{x_k\}$,

where $P_{N-1}(x, \vec{n})$ *is* $N-1$ *dimensional plane in* $\mathbb{R}^N$, $x \in P_{N-1}(x, \vec{n})$, $P_{N-1}(x, \vec{n}) \perp \vec{n}$, $1 \leqslant k \leqslant N-1$, $\{\vec{\tau}_k\}_1^{N-1}$ *is a basis in* $P_{N-1}(x, \vec{n})$.

Proof of the lemma is given in Appendix A.

Notice that in several space dimensions locally one dimensional approach is often used for building of computational algorithms, e.g., in finite volume framework. In line with this we replace (1.9) by the following requirement:

locally one dimensional equilibria are maintained. (1.13)

Definition 2. Numerical schemes possessing the properties (1.9), (1.10), (1.13) are called equilibrium type schemes.

Notice that equilibrium and equilibrium type schemes are equivalent in one dimension.

Convergence of the natural discretization of the source as $b(u(t^n, \vec{x_j})) \cdot \mathrm{div} z(\vec{x_j})$ is proved (see [8] for the explicit kinetic schemes and [29] for the splitting algorithm); but it is well-known and we will see later that the convergence to steady states is very slow. That is why construction and investigation of numerical schemes for conservation laws with source terms have been addressed by several authors. Upwind methods for the discretization of source term has been introduced by Bermudez and Vazqez [6] and then developed further in [5,42] for unstructured mesh for the shallow water equations. Also in Gascon and Corberan [19] equation with source term in single space dimension is written equivalently as homogenous equation by means of integration of the source with respect to independent space variable. Then special upwind discretization of space derivative is used that results in upwind discretization of source term. Well balanced schemes have been introduced by Greenberg et al. [23], and studied further in Greenberg-LeRoux et al. [24], Gosse-LeRoux [21], Gosse [22]. The convergence of these schemes is proved in one space dimension for scalar conservation laws with initial data possessing bounded variation. The method for balancing the source term in the framework of Godunov type schemes has been introduced by LeVeque [32] and applied to Euler equations with source terms [33]. Riemann solver developed in Jenny et al. [26] takes into account viscous and source terms. Kinetic schemes with equilibrium conservation properties have been introduced by Audusse et al. [3], Bristeau et al. [11], Perthame et al. [37] for Saint-Venant systems. Equilibrium schemes have been introduced in Botchorishvili et al. [7] and then have been extended as equilibrium type schemes to several space dimensions in [8]. The convergence of these methods is proved in the framework of kinetic schemes with L^∞ initial data [7,8]. In Botchorishvili [9] an implicit approach for building schemes with

equilibrium conservation property was studied. For shallow water equations special data reconstruction procedure is proposed in Zhou et al. [43]. The procedure uses gradient of water level instead of water depth and together with central cell centered discretization of source term ensures the so-called C-property; i.e., the scheme maintains certain equilibrium state defined as constant water level with zero velocity. In Jin [25] it is shown that even second order approximation of steady state equation in conservative form can significantly increase accuracy of computations. In finite difference framework correction procedure for compensating the errors in approximation of source term is developed in Smolarkevich et al. [39]. In Arvantis et al. [2] hyperbolic equations with stiff source terms are studied in the context of adaptive grids and finite elements.

In this paper we introduce a new class of equilibrium type finite volume schemes on arbitrary unstructured meshes that possess properties (1.9), (1.10), (1.13). Under some regularity requirement on mesh refinement we prove their convergence to entropy solutions of (1.1), (1.2) and we demonstrate their efficiency on a few numerical tests.

The paper is organized as follows. Section 2 is devoted to the construction of new equilibrium type schemes. First we formulate the principle of design of the schemes. Then we construct the schemes in one dimension and then in several space dimensions and we prove that they possess property (1.13).

In Section 3 we study the convergence of these new equilibrium type schemes in a kinetic framework, i.e., we consider the schemes with numerical flux functions admitting suitable interpretation at the kinetic level. We derive the properties of the scheme. Then we recall kinetic formulation of scalar conservation laws [34] and generalized kinetic solutions [7]. Related information on main convergence theorem for kinetic schemes [7] and on its appication is given in Appendix C. We also recall regular mesh refinement [8] and under this supposition on mesh refinement process we prove the convergence of our scheme to entropy solutions of (1.1), (1.2).

In Section 4 we present the numerical results. They show that the scheme works well for a variety of scalar conservation laws; it is far more accurate than the standard scheme, i.e., scheme with cell centered discretization of source term, and it needs much less nodal points to ensure a comparable accuracy. The effect of the various choices of finite volume cells for the same triangular meshes is studied as well. We have gathered numerical evidence that the rate of convergence of our equilibrium type scheme increases together with the refinement, while the rate of convergence of the standard scheme is below of 1 and close to zero. This means that equilibrium type schemes have some exponential type convergence. We also introduce a new numerical implementation for Dirichlet boundary conditions. Numerical tests show that our equilibrium type scheme in conjunction with the developed numerical model of boundary conditions produces accurate numerical results for initial-boundary value problems over domain with curvilinear geometry. In the last subsection a test problem with a Dirac mass in the source is considered. The standard scheme is unstable for this problem, while the equilibrium type scheme produces highly accurate approximate solutions.

In Section 5 we give formal extension of our algorithm for systems of conservation laws.

2. Construction of the schemes

2.1. Principle of design

Observe that

$$b(u) = \frac{\sum_{i=1}^{N} \frac{\partial A_i(u)}{\partial x_i}}{\sum_{i=1}^{N} \frac{\partial D_i(u)}{\partial x_i}}, \tag{2.1}$$

where D_i are defined by (1.7). In (1.1) substitution of $b(u)$ by its expression defined by (2.1) yields the following equation:

$$\frac{\partial u}{\partial t}+\sum_{i=1}^{N}\frac{\partial A_i(u)}{\partial x_i}+\frac{\sum_{i=1}^{N}\frac{\partial A_i(u)}{\partial x_i}}{\sum_{i=1}^{N}\frac{\partial D_i(u)}{\partial x_i}}\cdot\sum_{i=1}^{N}\frac{\partial z_i(x)}{\partial x_i}=0. \tag{2.2}$$

We propose that (2.2) is a suitable form of scalar conservation law (1.1) to perform discretization of source term in order to achieve high order precision at equilibrium states. Observe that if we are at equilibrium state, i.e.

$$\sum_{i=1}^{N}\frac{\partial A_i(u)}{\partial x_i}+b(u)\sum_{i=1}^{N}\frac{\partial z_i(x)}{\partial x_i}=0,$$

then (1.6) is valid and we have:

$$\sum_{i=1}^{N}\frac{\partial z_i(x)}{\partial x_i}=-\sum_{i=1}^{N}\frac{\partial D_i(u)}{\partial x_i}. \tag{2.3}$$

Then substitution of right-hand side of (2.3) in (2.2) yields:

$$\frac{\partial u}{\partial t}=-\left(\sum_{i=1}^{N}\frac{\partial A_i(u)}{\partial x_i}+\frac{\sum_{i=1}^{N}\frac{\partial A_i(u)}{\partial x_i}}{\sum_{i=1}^{N}\frac{\partial D_i(u)}{\partial x_i}}\cdot\left(-\sum_{i=1}^{N}\frac{\partial D_i(u)}{\partial x_i}\right)\right)=0, \tag{2.4}$$

i.e., $\partial u/\partial t=0$. We seek an algorithm, i.e., a discretization of (2.1), with the same property at the discrete level. Suppose that Ω_{jk} is a subelement of a mesh, e.g., a triangle in two dimensions, or an union of such subelements possessing one common node, e.g., a cell or some part of a cell. For clarity we set: $C_j=\cup\Omega_{jk}$, where C_j denotes a mesh cell. We formulate the following four steps algorithm for the construction of the scheme:

Algorithm

1. Perform a spatial discretization of $\sum_{i=1}^{N}\frac{\partial A_i(u)}{\partial x_i}$ on each cell C_j.
2. Find the corresponding discretization on each Ω_{jk} ensuring the following:

$$\sum_{i=1}^{N}\frac{\partial A_i(u)}{\partial x_i}\bigg|_{C_j}(x)=\frac{1}{|C_j|}\sum_{k}|\Omega_{jk}|\sum_{i=1}^{N}\frac{\partial A_i(u)}{\partial x_i}\bigg|_{\Omega_{jk}}(x),\quad x\in C_j.$$

3. Discretize (2.3) at the desired order of accuracy on each Ω_{jk};
4. Discretize the source term according to the following principle:

$$\begin{aligned}\int_{C_j}\frac{\sum_{i=1}^{N}\frac{\partial A_i(u)}{\partial x_i}}{\sum_{i=1}^{N}\frac{\partial D_i(u)}{\partial x_i}}\cdot\sum_{i=1}^{N}\frac{\partial z_i(x)}{\partial x_i}\,\mathrm{d}x&=\sum_{k}\int_{\Omega_{jk}}\frac{\sum_{i=1}^{N}\frac{\partial A_i(u)}{\partial x_i}}{\sum_{i=1}^{N}\frac{\partial D_i(u)}{\partial x_i}}\cdot\sum_{i=1}^{N}\frac{\partial z_i(x)}{\partial x_i}\,\mathrm{d}x\\&=\sum_{k}|\Omega_{jk}|\frac{\sum_{i=1}^{N}\frac{\partial A_i(u)}{\partial x_i}\Big|_{\Omega_{jk}}}{\sum_{i=1}^{N}\frac{\partial D_i(u)}{\partial x_i}\Big|_{\Omega_{jk}}}\cdot\sum_{i=1}^{N}\frac{\partial z_i(x)}{\partial x_i}\bigg|_{\Omega_{jk}}.\end{aligned} \tag{2.5}$$

Observe that by Step 3 the discrete steady states of the resulting scheme are defined by the relation:

$$\sum_{i=1}^{N} \frac{\partial z_i(x)}{\partial x_i}\bigg|_{\Omega_{jk}} = -\sum_{i=1}^{N} \frac{\partial D_i(u)}{\partial x_i}\bigg|_{\Omega_{jk}}. \tag{2.6}$$

By the same argument as in the continuous case it is easy to see that the resulting scheme preserves discrete steady states defined by (2.6).

Notice that the discretization of source term uses some arbitrary discretization of the steady state Eq. (1.6) and that is, at least formally, completely independent from the discretization of the space derivatives. Thus the algorithm can be used in conjunction with first and high order schemes, finite difference, finite element or spectral discretizations, explicit or implicit in time. Notice also that the algorithm presented above just uses Eq. (2.1) in order to rewrite Eq. (1.1) equivalently as Eq. (2.2) that is more appropriate for the discretization of source terms. Thus the above discretization algorithm is also valid outside of equilibria. Some examples of application of the algorithm are given in next subsections.

2.2. The scheme in one dimension

In this subsection we apply the algorithm given above and build schemes for one dimensional ($N = 1$) nonlinear scalar conservation laws. Therefore we drop the subscripts when appropriate.

We set $C_j = [x_{j-1/2}, x_{j+1/2}]$, $\Omega_{j,j-1} = [x_{j-1/2}, x_j]$, $\Omega_{j,j+1} = [x_j, x_{j+1/2}]$;

$$\frac{\partial A}{\partial x}\bigg|_{\Omega_{j,j-1}} = \frac{2}{\Delta x}\int_{x_{j-1/2}}^{x_j} \frac{\partial A}{\partial x}\,\mathrm{d}x = \frac{2}{\Delta x}(A_j - A_{j-1/2}) \approx \frac{2}{\Delta x}(A(u_j, u_j) - A(u_j, u_{j-1}));$$

$$\frac{\partial A}{\partial x}\bigg|_{\Omega_{j,j+1}} \approx \frac{2}{\Delta x}(A(u_{j+1}, u_j) - A(u_j, u_j));$$

$$\frac{\partial A}{\partial x}\bigg|_{C_j} = \frac{1}{\Delta x}\left(\frac{\Delta x}{2}\frac{\partial A}{\partial x}\bigg|_{\Omega_{j,j-1}} + \frac{\Delta x}{2}\frac{\partial A}{\partial x}\bigg|_{\Omega_{j,j+1}}\right) \approx \frac{1}{\Delta x}(A(u_{j+1}, u_j) - A(u_j, u_j)) + \frac{1}{\Delta x}(A(u_j, u_j) - A(u_j, u_{j-1}));$$

$$\frac{\partial D(u)}{\partial x}\bigg|_{\Omega_{j,j-1}} = \frac{2}{\Delta x}\int_{x_{j-1/2}}^{x_j} \frac{\partial D}{\partial x}\,\mathrm{d}x = \frac{2}{\Delta x}(Dj - D_{j-1/2}) \approx \frac{1}{\Delta x}(D(u_j) - D(u_{j-1}));$$

$$\frac{\partial D(u)}{\partial x}\bigg|_{\Omega_{j,j+1}} \approx \frac{1}{\Delta x}(D(u_{j+1}) - D(u_j));$$

$$\frac{\partial z(x)}{\partial x}\bigg|_{\Omega_{j,j+1}} \approx \frac{1}{\Delta x}(z_{j+1} - z_j); \quad \frac{\partial z(x)}{\partial x}\bigg|_{\text{for } \Omega_{j,j-1}} \approx \frac{1}{\Delta x}(z_j - z_{j-1}),$$

where $\Delta x = x_{j+1/2} - x_{j-1/2}$. Observe that discretizatins of $\partial z(x)/\partial x$ and $\partial D(u)/\partial x$ enable to exactly recover exact solutions of (2.3). Then first order monotone implicit equilibrium schemes write

$$\frac{u_j^{n+1} - u_j^n}{\Delta t} + \frac{A(u_{j+1}^{n+1}, u_j^{n+1}) - A(u_j^{n+1}, u_{j-1}^{n+1})}{\Delta x} + \frac{A(u_{j+1}^{n+1}, u_j^{n+1}) - A(u_j^{n+1}, u_j^{n+1})}{D(u_{j+1}^{n+1}) - D(u_j^{n+1})} \cdot \frac{z_{j+1} - z_j}{\Delta x}$$
$$+ \frac{A(u_j^n, u_j^n) - A(u_j^n, u_{j-1}^n)}{D(u_j^n) - D(u_{j-1}^n)} \cdot \frac{z_j - z_{j-1}}{\Delta x} = 0, \tag{2.7}$$

where the numerical flux function $A(u, v)$ is monotone, (see for e.g. [38]).

A variant of the above scheme can be obtained with different choice of $\Omega_{j,j\pm1}$ in the algorithm of discretization of source term, namely, if we do not use subdivision of the cell and set $\Omega_j = C_j$. Explicit variant of this scheme writes:

$$\frac{u_j^{n+1}-u_j^n}{\Delta t}+\frac{A(u_{j+1}^n,u_j^n)-A(u_j^n,u_{j-1}^n)}{\Delta x}+\frac{A(u_{j+1}^n,u_j^n)-A(u_j^n,u_{j-1}^n)}{D(u_{j+1}^n)-D(u_{j-1}^n)}\cdot\frac{z_{j+1}-z_{j-1}}{\Delta x}=0. \tag{2.8}$$

We can couple the approach for the constructing equilibrium schemes with high order monotone methods, such as MUSCL [41], e.g., such scheme writes:

$$u_j^{n+1}-u_j^n+\frac{\Delta t}{\Delta x}\Big(A(u_{j+1}^n-,u_j^n+)-A(u_j^n-,u_{j-1}^n+)\Big)+\Delta t\frac{A(u_{j+1}^n-,u_j^n+)-A(u_j^n-,u_{j-1}^n+)}{0.5(D(u_{j+1}^n)-D(u_{j-1}^n))}\cdot\frac{z_{j+1}-z_{j-1}}{2\Delta x}=0, \tag{2.9}$$

where the so-called reconstructed values satisfy

$$u_j^n\pm=u_j^n\pm\frac{\Delta x}{2}\cdot\sigma_x(x_j),\quad \sigma_x=u_{xx}(x_j^n)+0(\Delta x^2),$$

at least in the regions of smoothness and monotonicity, consult [20] and [31] for the several concrete choices of the limiters.

The following lemma is evident due to the principle of design of the above schemes:

Lemma 2.2.1. *The schemes* (2.7)–(2.9) *are exact on the equilibrium states of Eq.* (1.1), $N=1$, *defined by the following relation*:

$$D(u_{j+1})+z_{j+1}=D(u_j)+z_j. \tag{2.10}$$

Remark 2.1. All the above schemes are based on the formulae (2.1) for the representation of the function $b(u)$. This formulae is not valid when $a(s)=0$ and $b(s)\neq 0$ that implies $D'(s)=0$. At a discrete level, e.g., for the scheme (2.9), this is equivalent to the case when $D(u_{j+1})=D(u_{j-1})$. But according to the exact steady state Eq. (2.10) the latter can not occur at the equilibria unless $z(x_{j+1})=z(x_{j-1})$, i.e., when the equation is homogenous in corresponding subdomain. That is why in such nodes and cell interfaces we apply standard cell centered discretization of a source, see formulae (3.26), (3.27) and Remark 3.3 for details. We will see later in Section 4 that this approach works well in practise.

2.3. Multidimensional cell centered discretization of the source terms

For (1.1) the monotone finite volume scheme with standard cell center discretization of a source can be written as follows:

$$\frac{u_j^{n+1}-u_j^n}{\Delta t}+\sum_k\sum_l\frac{|\Gamma_{jk}^l|}{|C_j|}A(u_j^n,u_k^n,\vec{n}_{jk}^l)+\frac{b(u_j^n)}{|C_j|}\sum_k\sum_l|\Gamma_{jk}^l|\langle z(\vec{x_k}),\vec{n}_{jk}^l\rangle=0, \tag{2.11}$$

$$u_j^0=\frac{1}{|C_j|}\int_{C_j}u_0(x)\,\mathrm{d}x, \tag{2.12}$$

where $\langle\cdot,\cdot\rangle$ is a scalar product in $\mathbb{R}^N$, $A(u_j^n,u_k^n,\vec{n}_{jk})$ is a monotone numerical flux function [38] satisfying usual requirements on consistency:

$A(u,u,\vec{n})=\langle A(u),\vec{n}\rangle$,

$A(u,v,\vec{n})$ is Lifschitz continuous with respect to u,v,

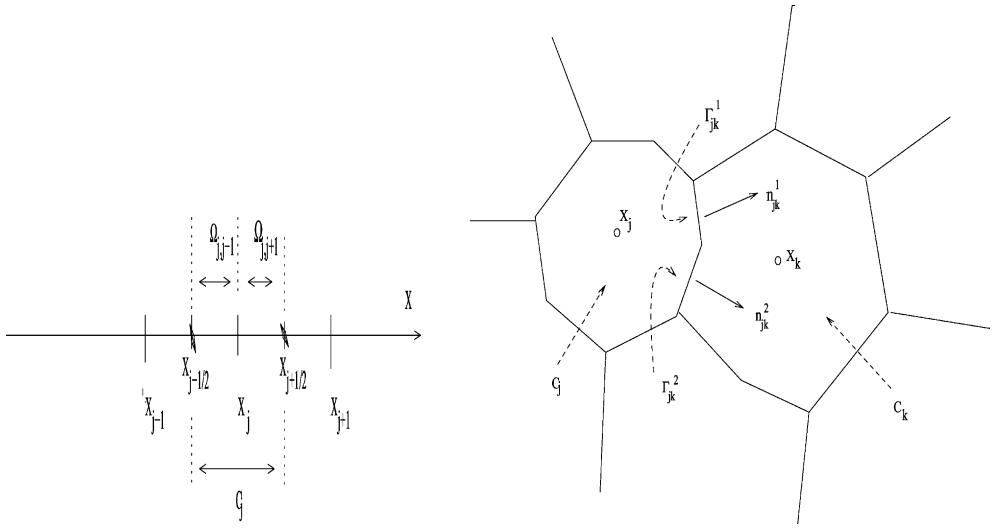

Fig. 1. Cells in one and two space dimensions.

and on monotonicity:

$A(u, v, \vec{n})$ is nondecreasing in u and nonincreasing in v;

u_j^n is approximate solution at time t_n in nodal point $\vec{x_j}$ of a mesh $\mathscr{T}$, $\vec{x_j} \in \mathbb{R}^N, j = 0, 1, \ldots$; as before C_j are cells associated with node $\vec{x_j}$ and Γ_{jk} is the interface between cells C_j and C_k, $\Gamma_{jk} = C_j \cap C_k$, $\Gamma_{jk} = \cup_l \Gamma_{jk}^l$, $\vec{n}_{jk}^l$ is the unit normal normal of Γ_{jk}^l directed into C_k, see also Fig. 1. Notice that cell interface Γ_{jk} can be composed by several subinterfaces Γ_{jk}^l, e.g., as in case of median based cell Definition [1]. Notice also that here and onward superscript l refers to subinterface number.

An example of monotone flux function is Engquist–Osher's [18] which writes for unstructured meshes

$$A(u, v, \vec{n}) = \int_0^u \max\left(0, \sum_{i=1}^N a_i(\xi) n_i\right) \mathrm{d}\xi + \int_0^v \min\left(0, \sum_{i=1}^N a_i(\xi) n_i\right) \mathrm{d}\xi. \tag{2.13}$$

2.4. Equilibrium type discretization of source term in several space dimensions

Observe that in one dimension we can integrate the steady state Eq. (1.6) explicitly in order to have equivalent finite difference formulation, i.e., Eq. (2.10). In several space dimensions this is not possible in general.

Observe that a local one dimensional approach would be in the line of finite volume method that uses the same idea for the construction of numerical flux functions at cell interfaces. Thus for explicit finite volume scheme, the analogue of (2.7) on unstructured meshes writes:

$$\frac{u_j^{n+1} - u_j^n}{\Delta t} + \frac{1}{|C_j|} \sum_k \sum_l |\Gamma_{jk}^l| A(u_j^n, u_k^n, \vec{n}_{jk}^l) + \sum_k \sum_l \frac{|\Gamma_{jk}^l|}{|C_j|} \frac{A(u_j^n, u_k^n, \vec{n}_{jk}^l) - A(u_j^n, u_j^n, \vec{n}_{jk}^l)}{\langle D(u_k^n), \vec{n}_{jk}^l \rangle - \langle D(u_j^n), \vec{n}_{jk}^l \rangle} \cdot \left(\langle z(\vec{x}_k), \vec{n}_{jk}^l \rangle - \langle z(\vec{x}_j), \vec{n}_{jk}^l \rangle \right) = 0, \tag{2.14}$$

where $z = (z_1, z_2, \ldots, z_N), D = (D_1, D_2, \ldots, D_N)$, D_i are defined by (1.7).

Proposition 2.4.1. *Finite volume scheme* (2.14) *is exact on locally one dimensional equilibrium states of Eq.* (1.1).

Proof. Under the assumptions of the lemma, equilibria of the Eq. (1.1) are defined by:

$$\langle D(u_k^n), \vec{n}_{jk}^l \rangle + \langle z(\vec{x}_k), \vec{n}_{jk}^l \rangle = \langle D(u_j^n), \vec{n}_{jk}^l \rangle + \langle z(\vec{x}_j), \vec{n}_{jk}^l \rangle. \tag{2.15}$$

Thus if we are at equilibrium (2.15) are satisfied. Observe that

$$\sum_k \sum_l \frac{|\Gamma_{jk}^l|}{|C_j|} A(u_j^n, u_j^n, \vec{n}_{jk}^l) = 0$$

according to the consistency property of the numerical flux function and the divergence theorem. Then extracting $\langle z(\vec{x}_k), \vec{n}_{jk} \rangle - \langle z(\vec{x}_j), \vec{n}_{jk} \rangle$ from (2.15) and substituting in (2.14) shows that $u_j^{n+1} = u_j^n$, i.e., locally one dimensional equilibrium data are maintained. □

Notice that standard scheme (2.11) discretizes source term in cell centers, i.e., using values at cell centers only. Our equilibrium type scheme discretizes source terms at cell interfaces and this discretization is edge based.

2.5. More accurate equilibrium type discretizations for arbitrary meshes

Observe that the equilibrium state in scheme (2.14) is defined by (2.15) and it is a true equilibrium under the assumptions of Lemma 2.4.1. Thus in general (2.15) is not a good approximation of (2.3). For meshes with median based cells a better accuracy for (2.3) can be achieved by the following:

$$\sum_k \sum_l \frac{|\Gamma_{jk}^l|}{2|C_j|} \left(\langle D(u_k^n) + D(u_j^n), \vec{n}_{jk}^l \rangle + \langle z(\vec{x}_k) + z(\vec{x}_j), \vec{n}_{jk}^l \rangle \right) = 0. \tag{2.16}$$

Namely (2.16) can be a second order approximation of (2.3) in the sense of the local truncation error for uniformly regular meshes. If in the algorithm for the building of the scheme we set $\Omega_{jk} = C_j$ then corresponding to (2.16) the finite volume scheme writes:

$$\frac{u_j^{n+1} - u_j^n}{\Delta t} + \frac{1}{|C_j|} \sum_k \sum_l |\Gamma_{jk}^l| A(u_j^n, u_k^n, \vec{n}_{jk}^l) + \frac{1}{|C_j|} \sum_k \sum_l \frac{\sum_k \sum_l |\Gamma_{jk}^l| A(u_j^n, u_k^n, \vec{n}_{jk}^l)}{\sum_k \sum_l |\Gamma_{jk}^l| \left\langle D(u_k^n) + D(u_j^n), \vec{n}_{jk}^l \right\rangle} \cdot \langle z(\vec{x}_k) + z(\vec{x}_j), \vec{n}_{jk}^l \rangle = 0. \tag{2.17}$$

Observe that other variants of the scheme with $\Omega_{jk} \neq C_j$ are possible as well. Notice that (2.17) can be put in a simple and usual form of monotone schemes for homogenous equation with local time step

$$u_j^{n+1} = u_j^n - \frac{\Delta t_j}{|C_j|} \sum_k \sum_l |\Gamma_{jk}^l| A(u_j^n, u_k^n, \vec{n}_{jk}^l), \tag{2.18}$$

where

$$\Delta t_j = \Delta t \left(1 + \frac{\sum_k \sum_l |\Gamma_{jk}^l| \langle z(\vec{x}_k) + z(\vec{x}_j), \vec{n}_{jk}^l \rangle}{\sum_k \sum_l |\Gamma_{jk}^l| \langle D(u_k^n) + D(u_j^n), \vec{n}_{jk}^l \rangle} \right). \tag{2.19}$$

Notice that under the assumption of Lemma 2.4.1 the scheme (2.18), (2.19) is also equilibrium conserving. Observe that the approach enables us to decouple discretization of the steady state equation from those of the space derivatives. Thus high order accurate (at equilibrium states) numerical schemes for arbitrary meshes should be easy to build: one needs only to replace (2.16) by higher order approximations of (1.6). Clearly this is a formal construction and each scheme requires to be investigated separately but that is beyond the scope of the present paper. Here we only give an example of the "local time step" of such second order scheme

$$\Delta t_j = \Delta t\left(1+\frac{\sum_k \sum_l |\Gamma^l_{jk}|\langle z(\vec{x}^l_{jk}),\vec{n}^l_{jk}\rangle}{\sum_k \sum_l |\Gamma^l_{jk}|\langle D(u^{nl}_{jk}),\vec{n}^l_{jk}\rangle}\right), \tag{2.20}$$

where $\vec{x}^l_{jk}$ is a center of Γ^l_{jk} ensuring that simple midpoint numerical integration formulae is exact for linear functions.

3. Convergence of the schemes

In this section we study those equilibrium type schemes the numerical flux functions of which admit interpretation in the framework of kinetic schemes (see [36] for details related to the kinetic schemes). For scalar conservation laws such numerical flux functions verify:

$$A(u,v,\vec{n}^l_{jk}) = \int_0^u \alpha^l_{jk,+}(\xi)\,\mathrm{d}\xi + \int_0^v \alpha^l_{jk,-}(\xi)\,\mathrm{d}\xi, \tag{3.1}$$

where

$$\alpha^l_{jk,+}(\xi)\geqslant 0,\quad \alpha^l_{jk,-}(\xi)\leqslant 0,\quad \alpha^l_{jk,+}(\xi)+\alpha^l_{jk,-}(\xi)=\left\langle \vec{a}(\xi),\ \vec{n}^l_{jk}\right\rangle.$$

We also suppose that for the mesh $\mathscr{T}$ a minimum angle condition is satisfied (that is a usual requirement for finite element meshes for conservation laws). This means that each nodal point $\vec{x_j}$ is surrounded maximum of K_n neighbor nodes $\vec{x_k}$ for which $C_j\cap C_k\neq\emptyset$ holds true. Notice that the cell interface between nodes j and k can be composed by several subinterfaces as it is in Fig. 1. We suppose that each interface can consist of maximum $l_{\max}$ subinterfaces. Then any cell can have maximum $K=K_n l_{\max}$ subinterfaces. We set

$$\Delta x_{\min}=\min_j \min_{(k,\Gamma_{jk}\neq\emptyset)}\frac{|C_j|}{|\Gamma_{jk}|},\quad \Delta x=\max_j\max_{(k,\Gamma_{jk}\neq\emptyset)}\left(\frac{|C_j|}{|\Gamma_{jk}|},|\vec{x_j}-\vec{x_k}|\right),$$

and suppose that there exists such $\delta_{\mathscr{T}}$ that $(\Delta x/\Delta x_{\min})\leqslant\delta_{\mathscr{T}}$. Notice that this condition ensures $|C_i|/|C_j|\leqslant\delta_{\mathscr{T}}$, $(|\Gamma_{jk}|/|C_j|)|\vec{x_j}-\vec{x_k}|\leqslant\delta_{\mathscr{T}}$.

3.1. Properties of the scheme

Recall that if $D(u_k)=D(u_j)$ then in practise we replace equilibrium type discretization of a source by the standard cell centered discretization, see Remark 2.1. Since the properties of standard cell centered discretization are known, see e.g. [9], we assume $D(u_k)\neq D(u_j)$ throughout this subsection and study the properties of our equilibrium type scheme (2.14).

3.1.1. L^∞ estimate

Proposition 3.1.1. *Assume that*

1. $u_0 \in L^\infty(\mathbb{R}^N)$,
2. (1.3) *is satisfied*,
3. $$\frac{|\alpha^l_{jk,-}(\xi)|}{|\langle D(\xi), \vec{n}^l_{jk}\rangle|} \leqslant K_a|\xi|, \tag{3.2}$$
4. *CFL condition*

$$\frac{\Delta t}{\Delta x_{\min}} \max_j \max_{|\xi|\leqslant K_\infty} \sum_k \sum_l |\langle \vec{a}(\xi), \vec{n}^l_{jk}\rangle| \leqslant 1, \tag{3.3}$$

$$K_\infty = \exp(T \cdot K \cdot K_a \cdot \delta_{\mathscr{T}} K_z) \cdot |u_0|_{L^\infty},$$

holds true.

Then the numerical scheme (2.14) *satisfy*

$$|u^n_j| \leqslant K_a, \quad n \leqslant \frac{T}{\Delta t}. \tag{3.4}$$

Proof. We set:

$$q = \frac{A(u^n_j, u^n_k, \vec{n}^l_{jk}) - A(u^n_j, u^n_j, \vec{n}^l_{jk})}{\langle D(u^n_k) - D(u^n_j), \vec{n}^l_{jk}\rangle}, \tag{3.5}$$

$$\Phi(y) = A(u^n_j, y \cdot u^n_k + (1-y) \cdot u^n_j, \vec{n}^l_{jk}) - q \cdot \langle D(y \cdot u^n_k + (1-y) \cdot u^n_j), \vec{n}^l_{jk}\rangle. \tag{3.6}$$

From (3.5), (3.6) we obtain:

$$\begin{aligned} &\Phi(1) - \Phi(0) = A(u^n_j, u^n_k, \vec{n}^l_{jk}) - A(u^n_j, u^n_j, \vec{n}^l_{jk}) - q \cdot \langle D(u^n_k) - D(u^n_j), \vec{n}^l_{jk}\rangle, \\ &0 = \Phi(1) - \Phi(0) = \Phi'(\theta^n_{jkl}), \quad 0 < \theta^n_{jkl} < 1. \end{aligned} \tag{3.7}$$

From (3.6), (3.7) we easily compute

$$q = \frac{\alpha^l_{jk,-}(\xi^n_{jkl})}{\langle D'(\xi^n_{jkl}), \vec{n}^l_{jk}\rangle},$$

i.e., we have:

$$\frac{A(u^n_j, u^n_k, \vec{n}^l_{jk}) - A(u^n_j, u^n_j, \vec{n}^l_{jk})}{\langle D(u^n_k) - D(u^n_j), \vec{n}^l_{jk}\rangle} = \frac{\alpha^l_{jk,-}(\xi^n_{jkl})}{\langle D'(\xi^n_{jkl}), \vec{n}^l_{jk}\rangle}, \tag{3.8}$$

where $\xi^n_{jkl} = \theta^n_{jkl} u^n_j + (1-\theta^n_{jkl}) u^n_k$ for some $0 < \theta^n_{jkl} < 1$. According to (3.2) the expression (3.8) is bounded by $K_a|\xi|$. Thus source term of the equilibrium type scheme (2.14) can be controlled as follows

$$\left|\sum_k\sum_l \frac{|\Gamma_{jk}^l|}{|C_j|}\frac{A(u_j^n,u_k^n,\vec{n}_{jk}^l)-A(u_j^n,u_j^n,\vec{n}_{jk}^l)}{\langle D(u_k^n),\vec{n}_{jk}^l\rangle-\langle D(u_j^n),\vec{n}_{jk}^l\rangle}\cdot\Big(\langle z(\vec{x}_k),\vec{n}_{jk}^l\rangle-\langle z(\vec{x}_j),\vec{n}_{jk}^l\rangle\Big)\right|$$

$$\leqslant \sum_k\sum_l \frac{|\Gamma_{jk}^l|}{|C_j|}K_a\cdot|\xi_{jk}^l|\cdot K_z\cdot|\vec{x_j}-\vec{x_k}|\leqslant K\cdot K_a\cdot K_z\cdot\delta_{\mathscr{T}}\cdot\max_j|u_j^n|. \tag{3.9}$$

Then using the standard technique on derivation of L^∞ bound for finite volume schemes, see e.g., [7,38], we have the following estimate:

$$|u_j^{n+1}|\leqslant(1+\Delta tK\cdot K_a\cdot K_z\cdot\delta_{\mathscr{T}})\cdot\max_j|u_j^n|.$$

The latter results in the validity of (3.4). □

Remark 3.1. Observe that the requirement (3.2) is satisfied by Engquist–Osher numerical flux function (2.13), since

$$\frac{|\alpha_{jk,-}^l(\xi)|}{|\langle D'(\xi),\vec{n}_{jk}^l\rangle|}=\frac{|\langle a_-(\xi),\vec{n}_{jk}^l\rangle|}{|\langle a(\xi),\vec{n}_{jk}^l\rangle|}|b(\xi)|\leqslant K_b|\xi|.$$

3.1.2. Entropy inequality

The scheme (2.14) is also written as

$$\frac{v_{1j}^{n+1}-u_j^n}{2\Delta t}+\sum_k\sum_l\frac{|\Gamma_{jk}^l|}{|C_j|}A(u_j^n,u_k^n,\vec{n}_{jk}^l)=0, \tag{3.10}$$

$$\frac{v_{2j}^{n+1}-u_j^n}{2\Delta t}+\sum_k\sum_l\frac{|\Gamma_{jk}^l|}{|C_j|}\frac{A(u_j^n,u_k^n,\vec{n}_{jk}^l)-A(u_j^n,u_j^n,\vec{n}_{jk}^l)}{\langle D(u_k^n),\vec{n}_{jk}^l\rangle-\langle D(u_j^n),\vec{n}_{jk}^l\rangle}\langle z(\vec{x}_k)-z(\vec{x}_j),\vec{n}_{jk}^l\rangle=0, \tag{3.11}$$

$$u_j^{n+1}=0.5\cdot(v_{1j}^{n+1}+v_{2j}^{n+1}).$$

On account of (3.9) we have the estimate:

$$|v_{2j}^{n+1}-u_j^n|\leqslant K\cdot K_a\cdot K_z\cdot\delta_{\mathscr{T}}\cdot K_\infty. \tag{3.12}$$

Because of the monotonicity of the numerical flux function under the CFL condition (3.3) we have for (3.10) the following in cell entropy inequality:

$$\frac{S(v_{1j}^{n+1})-S(u_j^n)}{2\Delta t}+\frac{1}{|C_j|}\sum_k\sum_l|\Gamma_{jk}^l|\eta(u_j^n,u_k^n,\vec{n}_{jk}^l)\leqslant 0, \tag{3.13}$$

where the entropy S is an arbitrarily smooth and convex function and η is the corresponding entropy flux function,

$$\eta(u,v,\vec{n}_{jk}^l)=\int_0^u S'(\xi)\alpha_{jk,+}^l(\xi)\,\mathrm{d}\xi+\int_0^v S'(\xi)\alpha_{jk,-}^l(\xi)\,\mathrm{d}\xi. \tag{3.14}$$

For (3.11) we have

$$\begin{aligned}\frac{S(v_{2j}^{n+1})-S(u_j^n)}{2\Delta t} &= \frac{S'(\zeta_{jkl}^{n+1/2})u_j^n)}{2\Delta t}(v_{2j}^{n+1}-u_j^n)\\ &= -S'(\zeta_{jkl}^{n+1/2})\sum_k\sum_l \frac{|\Gamma_{jk}^l|}{|C_j|}\frac{A(u_j^n,u_k^n,\vec{n}_{jk}^l)-A(u_j^n,u_j^n,\vec{n}_{jk}^l)}{\langle D(u_k^n)-D(u_j^n),\vec{n}_{jk}^l\rangle}\langle z(\vec{x}_k)-z(\vec{x}_j),\vec{n}_{jk}^l\rangle\\ &= -S'(u_j^n)\frac{1}{|C_j|}\sum_k\sum_l |\Gamma_{jk}^l|\frac{A(u_j^n,u_k^n,\vec{n}_{jk}^l)-A(u_j^n,u_j^n,\vec{n}_{jk}^l)}{\langle D(u_k^n)-D(u_j^n),\vec{n}_{jk}^l\rangle}\langle z(\vec{x_k})-z(x_j),\vec{n}_{jk}^l\rangle+\psi_{sj}^n,\end{aligned} \tag{3.15}$$

where $0\leqslant\theta_j^{n+1/2}\leqslant 1$, $\zeta_{jkl}^{n+1/2}=(1-\theta_j^{n+1/2})v_{2j}^{n+1}+\theta_j^{n+1/2}u_j^n$,

$$\psi_{sj}^n=(S'(u_j^n)-S'(\zeta_{jkl}^{n+1/2}))\sum_k\sum_l\frac{|\Gamma_{jk}^l|}{|C_j|}\frac{A(u_j^n,u_k^n,\vec{n}_{jk}^l)-A(u_j^n,u_j^n,\vec{n}_{jk}^l)}{\langle D(u_k^n)-D(u_j^n),\vec{n}_{jk}^l\rangle}\langle z(\vec{x}_k)-z(\vec{x}_j),\vec{n}_{jk}^l\rangle.$$

Observe that in this formulae the sums can be estimated according to (3.9). For the first multiplier we have

$$S'(u_j^n)-S'(\zeta_{jkl}^{n+1/2})=S''(\xi_{jkl}^{n+1/2})(u_j^n-\zeta_{jkl}^{n+1/2})=S''(\xi_{jkl}^{n+1/2})\cdot(1-\theta_j^{n+1/2})\cdot(v_{2j}^{n+1}-u_j^n),$$

where $\min(u_j^n,\zeta_{jkl}^{n+1/2})<\xi_{jkl}^{n+1/2}<\max(u_j^n,\zeta_{jkl}^{n+1/2})$. Notice that $v_{2j}^{n+1}-u_j^n$ can be controlled according to formulae (3.12). Thus on account of these estimates we obtain:

$$|\psi_{sj}^n|\leqslant(K\cdot K_a\cdot K_z\cdot\delta_{\mathscr{T}}\cdot K_\infty)^2\max_{|u|_{L^\infty}\leqslant K_\infty}S''(u)\cdot\Delta t. \tag{3.16}$$

With account of convexity of S and 3.10–3.16 we have the following in cell entropy inequality at macroscopic level:

$$\begin{aligned}&\frac{S(u_j^{n+1})-S(u_j^n)}{\Delta t}+\frac{1}{|C_j|}\sum_k\sum_l|\Gamma_{jk}^l|\eta(u_j^n,u_{k,l}^n,\vec{n}_{jk}^l)\\ &\quad+\frac{S'(u_j^n)}{|C_j|}\sum_k\sum_l|\Gamma_{jk}^l|\frac{A(u_j^n,u_k^n,\vec{n}_{jk}^l)-A(u_j^n,u_j^n,\vec{n}_{jk}^l)}{\langle D(u_k^n)-D(u_j^n),\vec{n}_{jk}^l\rangle}\langle z(\vec{x_k})-z(x_j),\vec{n}_{jk}^l\rangle-\psi_{sj}^n\leqslant 0,\end{aligned} \tag{3.17}$$

where ψ_{sj}^n vanishes together with time step.

The following proposition is a direct consequence of the above cell entropy inequality, Propositions 2.4.1 and 3.1.1.

Proposition 3.1.2. *Assume that* $u_0\in L^\infty(\mathbb{R}^N)$, (1.3), (3.2) are satisfied and the CFL condition (3.3) *holds true. Then numerical scheme* (2.14) *is equilibrium type scheme in the sense of* (1.9), (1.10), (1.13).

3.2. Preliminaries

The first general method of proof of the convergence of numerical schemes has been introduced by Kuznetsov [28]. The essential feature of this method is that it uses the doubling of variables technique at the finite difference level introduced by Kruzkov [27] for the uniqueness study of entropy solutions for scalar conservation laws. Doubling of the variables technique has been used by several authors for the proof of the convergence of variety of numerical schemes, (see e.g. [12,13,15,38]).

Notice that different approaches exist as well: see Szepessy [40] for scalar conservation laws in single space dimension, Coquel and Lefloch [14] in several space dimensions, Depres et al. [16] for linear advection

on arbitrary meshes. All these methods use some BV, weak BV or LV estimates in several space dimensions. Method of proof that needs only uniform L^∞ estimate in order to ensure suitable compactness framework does exist also. It is based on a kinetic formulation of scalar conservation laws (Lions, Perthame, Tadmor [34]), on the main convergence theorem of Botchorishvili, Perthame, Vasseur [7] and on regular mesh refinement [8]. We briefly recall the latters in the next subsections and in Appendix D.

3.2.1. Kinetic formulation

Kinetic formulation of scalar conservation laws and related equations has been introduced by Lions et al. [34]. This approach enables us to rewrite Eq. (1.1) and the family of entropy inequalities (1.4) as a single kinetic equation with a "density" function $\chi(\xi; u(t,x))$,

$$\chi(\xi;u)=\begin{cases}+1, & 0<\xi\leqslant u,\\ -1, & u\leqslant\xi<0,\\ 0, & \text{otherwise.}\end{cases} \tag{3.18}$$

Kinetic formulation is very useful since it simplifies analysis of the problem; e.g., it allows a very simple uniqueness proof [35]. In [7] the notion of kinetic solutions has been introduced; for (1.1) it writes:

Definition 3.1. Let $f(t,x,\xi)$ belongs to $L^\infty(0,T;L^\infty(\mathbb{R}^{N+1}_{x,\xi})\cap L^1(\mathbb{R}^{N+1}_{x,\xi}))$ for all $T\geqslant 0$. It is a "generalized kinetic solution" to (1.1), if

$$\frac{\partial f(t,x,\xi)}{\partial t}+\sum_{i=1}^{N}a_i(\xi)\cdot\frac{\partial f(t,x,\xi)}{\partial x_i}-\sum_{i=1}^{N}b(\xi)\cdot\frac{\partial f(t,x,\xi)}{\partial\xi}\cdot\frac{\partial z_i(x)}{\partial x_i}=\frac{\partial m(t,x,\xi)}{\partial\xi}, \tag{3.19}$$

in the sense of distribution for some nonnegative measure $m(t,x,\xi)$ bounded on $[0,T]\times\mathbb{R}^N_x\times\mathbb{R}_\xi$ for all $T>0$ which satisfies

$$0\leqslant \operatorname{sign}(\xi)f(t,x,\xi)=|f(t,x,\xi)|\leqslant 1, \tag{3.20}$$

$$\frac{\partial f}{\partial\xi}=\delta(\xi)-v(t,x,\xi), \tag{3.21}$$

with $v(t,x,\xi)$ some non negative measure such that $\int_{\mathbb{R}}v(t,x,\xi)\,\mathrm{d}\xi=1$ for all t,x.

It is easy to see that entropy solutions by Kruzkov [27] and Lax [30] and measure valued solutions by DiPerna [17] can be interpreted in the framework of generalized kinetic solutions [7]. The uniqueness of generalized kinetic solutions has been proved for conservation laws with source term [7]. The variant of the theorem in several space dimensions is given in Appendix D.

3.2.2. Regular refinement

It is known that for arbitrary meshes, finite volume discretization of space derivatives provides low order of accuracy only. Even in one dimension with numerical solution uniformly bounded but non smooth, it is impossible to have suitable discrete integration by parts formulae, see e.g. [8]. But this can be achieved under some hypotheses on the mesh refinement process. Namely, in order to use the main convergence theorem stated above the following definition of mesh regularity has been introduced in [8]:

Definition 3.2. Mesh $\mathscr{T}$ is γ-regular, if

$$\left\|\frac{1}{|C_j|}\mathscr{R}_{j\Delta x}(\mathscr{T},\xi)\right\|\leqslant K_R\Delta x^\gamma, \tag{3.22}$$

where K_R is some positive constant,

$$\mathscr{R}_{j\Delta x}(\mathscr{T},\xi)=\sum_k\sum_l|\Gamma^l_{jk}|\left(\langle\vec{a}(\xi),\vec{n}^l_{jk}\rangle(\vec{\vec{x}}^l_{jk}-0.5(\vec{x}_j+\vec{x}_k))+\frac{|\langle\vec{a}(\xi),\vec{n}^l_{jk}\rangle|}{2}(\vec{x_j}-\vec{x}_k)\right). \tag{3.23}$$

Notice that in two space dimensions uniform rectangular meshes with square cells and uniform triangular meshes with standard hexagonal cell definition are the simplest examples of meshes admitting regular refinement in the sense of Definition 3.2, (see Fig. 2). It is easy to see that $\mathscr{R}_{\Delta x}(\mathscr{T},\xi)$ defined by (3.23) is equal to zero for these meshes. For cartesian meshes smooth deformation of order $\Delta x^{1+\gamma}$ in each coordinate direction provide examples of nonuniform meshes with γ regularity property. E.g. to have γ-regularity of nonuniform cartesian meshes we can set

$$x^i_{j+1}-x^i_{j+1}=x^i_j-x^i_{j-1}+\beta_{j-1/2}|x^i_j-x^i_{j-1}|^{1+\gamma},\quad 1\leqslant i\leqslant N,\ \ |\beta_{j-1/2}|\leqslant K.$$

Observe that $\mathscr{R}_{\Delta x}(\mathscr{T},\xi)$ is Lifschitz continuous with respect to nodal points. Thus the suitable displacement of the nodes of uniform mesh at the distance $\kappa\Delta x^{1+\gamma}$ ensures that the resulting nonuniform mesh possesses γ the regularity property with some constant $K_{\kappa\gamma}$ (see Fig. 3 for examples of such nonuniform meshes). Furthermore, convergence theorem stated in previous subsection enables us not to respect mesh regularity requirement on the subdomains which have N-dimensional Lebesgue measure zero in the limit $\Delta x\to 0$. Thus we are allowed to perform local mesh refinement in frames of γ regularity, see an example in Fig. 4.

Lemma 3.2.1 (Sufficient condition of γ regularity [8]). *If*

$$\left|a(\xi)-\frac{1}{2|C_j|}\sum_k\sum_l|\Gamma^l_{jk}|\langle\vec{a}(\xi),\vec{n}^l_{jk}\rangle x_k\right|\leqslant K_1\Delta x^{\gamma}, \tag{3.24}$$

$$\left|\vec{x}_j-\frac{\sum_k\sum_l|\Gamma^l_{jk}|\cdot|\langle\vec{a}(\xi),\vec{n}^l_{jk}\rangle|\vec{x}_k}{\sum_k\sum_l|\Gamma^l_{jk}|\cdot|\langle\vec{a}(\xi),\vec{n}^l_{jk}\rangle|}\right|\leqslant K_2\Delta x^{1+\gamma}, \tag{3.25}$$

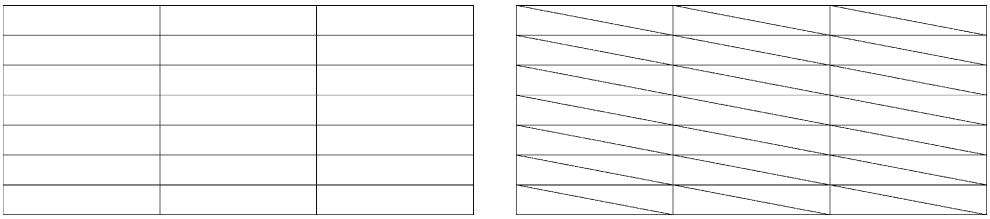

Fig. 2. Uniform rectangular and triangular meshes.

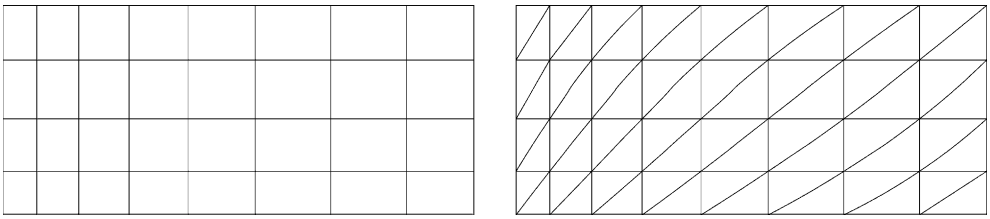

Fig. 3. Nonuniform smooth rectangular and triangular meshes.

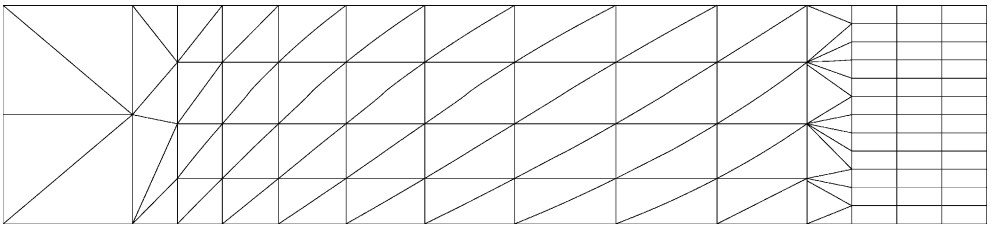

Fig. 4. Composite mesh with local refinement and derefinement.

then mesh $\mathscr{T}$ *is* γ *regular with* $K_R = K_1 + K_3 \cdot K_2 \cdot \delta_{\mathscr{T}}$,

$$K_3 = \frac{1}{2} \max_{|\xi| \leqslant |u_0|} \left(\sum_k \sum_l |\langle \vec{a}(\xi), \vec{n}^l_{jk} \rangle| \right).$$

Finally observe that for a given mesh $\mathscr{T}$ one can always determine suitable constant K_R in a such way that (3.24), (3.25) will be satisfied. Thus one can consider (3.22) as a requirement towards mesh refinement process: it does not accept such mesh refinement that will destroy regularity of initial mesh.

3.3. Convergence theorem

Observe that equilibrium type scheme (2.14) discretizes source term at cell interfaces in nonlinear manner that does not allow, in general, to have appropriate kinetic interpretation, i.e., suitable for the treatment in the L^∞ weak* compactness framework. That is why we modify discretization of source term. The modified scheme writes:

$$\frac{u_j^{n+1} - u_j^n}{\Delta t} + \frac{1}{|C_j|} \sum_k \sum_l |\Gamma^l_{jk}| A(u_j^n, u_k^n, \vec{n}^l_{jk}) + \sum_k \sum_l b^l_{jk} \frac{|\Gamma^l_{jk}|}{|C_j|} \Big(\langle z(\vec{x}_k), \vec{n}^l_{jk} \rangle - \langle z(x_j), \vec{n}^l_{jk} \rangle \Big) = 0, \tag{3.26}$$

where

$$b^l_{jk} = \begin{cases} \bar{b}^l_{jk} & \text{if } \max_{\xi \in I^l_{jk}} \alpha^l_{jk-}(\xi) \leqslant -\Delta x^{\gamma_b} \text{ and } |\sum_{1zj} / \sum_{zj}| \leqslant K_s, \\ b(u_j^n) & \text{otherwise,} \end{cases} \tag{3.27}$$

K_s, γ_b are some fixed constants, $0 < \gamma_b < 1$, $K_s > 0$,

$$\bar{b}^l_{jk} = \frac{A(u_j^n, u_k^n, \vec{n}^l_{jk}) - A(u_j^n, u_j^n, \vec{n}^l_{jk})}{\langle D(u_k^n), \vec{n}^l_{jk} \rangle - \langle D(u_j^n), \vec{n}^l_{jk} \rangle}, \tag{3.28}$$

$$I^l_{jk} = \Big(\min(u_k^n, u_k^n - g^l_{jk} K_a K_\infty K_z \Delta x^{1-\gamma_b}), \max(u_k^n, u_k^n - g^l_{jk} K_a K_\infty K_z \Delta x^{1-\gamma_b}) \Big), \tag{3.29}$$

$$g^l_{jk} = \operatorname{sign}(\bar{b}^l_{jk} \cdot \langle z_k - z_j, \vec{n}^l_{jk} \rangle) \tag{3.30}$$

$$\sum_{1zj} = \sum_{k, l \in I^l_{zjk}} \frac{|\Gamma^l_{jk}|}{|C_j|} \Big(\langle z(x_k), \vec{n}^l_{jk} \rangle - \langle z(x_j), \vec{n}^l_{jk} \rangle \Big), \tag{3.31}$$

$$\sum_{zj} = \sum_k \sum_l \frac{|\Gamma^l_{jk}|}{|C_j|}\Big(\langle z(x_k), \vec{n}^l_{jk}\rangle - \langle z(x_j), \vec{n}^l_{jk}\rangle\Big), \tag{3.32}$$

$$I^l_{zjk} = \left\{k, l : \max_{\xi \in I^l_{jk}} \alpha^l_{jk-} > -\Delta x^{\gamma_b}\right\}. \tag{3.33}$$

Remark 3.2. (3.26) has the same equilibrium conservation property as (2.14) but this property may be lost in the neighborhoods of the points where $\alpha^l_{jk-}(u^n_k) = 0$.

Lemma 3.3.1. *Assume that* $u_0 \in L^\infty(\mathbb{R}^N)$, (1.3), (3.2), (3.3) *are satisfied. Then numerical scheme* (3.26), (3.27) *equivalently writes*:

$$\frac{u^{n+1}_j - u^n_j}{\Delta t} + \frac{1}{|C_j|}\sum_k \sum_l |\Gamma^l_{jk}| A(u^n_j, u^n_{kl-}, \vec{n}^l_{jk}) + b_{sj}\sum_k \sum_l \frac{|\Gamma^l_{jk}|}{|C_j|}\Big(\langle z(\vec{x}_k), \vec{n}^l_{jk}\rangle - \langle z(x_j), \vec{n}^l_{jk}\rangle\Big) = 0, \tag{3.34}$$

$$b_{sj} = b(u^n_j)\cdot \frac{\sum_k \sum_l (1 - \operatorname{sign}(b(u^n_j) - b^l_{jk}))\Big(\langle z(\vec{x}_k), \vec{n}^l_{jk}\rangle - \langle z(\vec{x}_j), \vec{n}^l_{jk}\rangle\Big)}{\sum_{zj}}, \quad u^n_{kl-} = u^n_k \quad \text{if } b^l_{jk} = b(u^n_j).$$

Proof. Under assumptions of the lemma Proposition 3.1.1 is valid. Thus we have uniform L^∞ estimate (3.4) and we can write:

$$\left|\tilde{b}^l_{jk}\langle z_k - z_j, \vec{n}^l_{jk}\rangle\right| \leqslant K_a K_\infty K_z \Delta x, \tag{3.35}$$

where $\tilde{b}^l_{jk}$ is defined by (3.28). We set:

$$\varphi(y) = A(u_j, y, \vec{n}^l_{jk}) - A(u_j, u_k, \vec{n}^l_{jk}) - \tilde{b}^l_{jk}\langle z_k - z_j, \vec{n}^l_{jk}\rangle.$$

Notice that

$$A(u_j, y, \vec{n}^l_{jk}) - A(u_j, u_k, \vec{n}^l_{jk}) = \alpha^l_{jk-}(v)(y - u_k), \min(y, u_k) < v < \max(y, u_k),$$

and $\alpha^l_{jk-}(v) < -\Delta x^\gamma$ if $y \in I^l_{jk}$. We compute:

$$\begin{aligned}
&\varphi(u_k) = -\tilde{b}^l_{jk}\langle z_k - z_j, \vec{n}^l_{jk}\rangle,\\
&\varphi(u_k - g^l_{jk}K_a K_\infty K_z \Delta x^{1-\gamma_b}) = \alpha^l_{jk-}(v)\cdot(-g^l_{jk}K_a K_\infty K_z \Delta x^{1-\gamma_b}) - \tilde{b}^l_{jk}\langle z_k - z_j, \vec{n}^l_{jk}\rangle\\
&\qquad = -g^l_{jk}(\alpha^l_{jk-}(v)(K_a K_\infty K_z \Delta x + |\tilde{b}^l_{jk}\langle z_k - z_j, \vec{n}^l_{jk}\rangle|).
\end{aligned}$$

Observe that $v \in I^l_{jk}$ and therefore

$$\alpha^l_{jk-}(v) K_a K_\infty K_z \Delta x^{1-\gamma_b} < -K_a K_\infty K_z \Delta x.$$

With account of the latter inequality we have:

$$\operatorname{sign}(\varphi(u_k - g^l_{jk}K_a K_\infty K_z \Delta x^{1-\gamma_b})) = g^l_{jk}, \quad \operatorname{sign}(\varphi(u_k)) = -g^l_{jk},$$

i.e., φ changes the sign on I^l_{jk}. Because $\varphi(y)$ is a continuous function the equation $\varphi(y)=0$ has a solution $u^l_{jk-}\in I^l_{jk}$,

$$A(u_j,u^l_{jk-},\vec{n}^l_{jk})=A(u_j,u_k,\vec{n}^l_{jk})+\tilde{b}^l_{jk}\langle z_k-z_j,\vec{n}^l_{jk}\rangle.$$

Extracting $A(u_j,u_k,\vec{n}^l_{jk})$ from the latter equation and substituting it into (3.26) with account of (3.27) yields (3.34). □

Remark 3.3. Numerical scheme (3.34) can be interpreted as kinetic scheme

$$\frac{\chi^{n+1}_j(\xi)-\chi^n_j(\xi)}{\Delta t}+\frac{1}{|C_j|}\sum_k\sum_l\left(|\Gamma^l_{jk}|\alpha^l_{jk,+}(\xi)\chi^n_j(\xi)+|\Gamma^l_{jk}|\alpha^l_{jk,-}(\xi)\chi_{u^n_{jk,l-}}(\xi)\right)$$
$$+b_s(\xi)\cdot\frac{\partial\chi^n_j(\xi)}{\partial\xi}\cdot\frac{1}{|C_j|}\times\sum_k\sum_l|\Gamma^l_{jk}|\langle z_k-z_j,\vec{n}^l_{jk}\rangle=\frac{\partial\tilde{m}^{n+1}_j(\xi)}{\partial\xi},\tag{3.36}$$

where $\alpha^l_{jk,\pm}$ are defined according to (3.1), $\chi^n_j(\xi)=\chi(\xi;u^n_j)$, $\chi^n_{jk,l-}(\xi)=\chi(\xi;u^n_{jk,l-})$,

$$\frac{\partial\tilde{m}^{n+1}_j(\xi)}{\partial\xi}=\frac{\chi^{n+1}_j(\xi)-f^{n+1}_j(\xi)}{\Delta t},\tag{3.37}$$

and solution at macroscopic level is recovered according to the formula $u^{n+1}_j=\int_{\mathbb{R}_\xi}f^{n+1}_j(\xi)\,\mathrm{d}\xi$.

Theorem 3.3.2. *Assume that* $u_0\in L^\infty(\mathbb{R}^N)$, (1.3), (3.2), (3.3) are satisfied Then approximate solution $u_{\Delta x}(t,x)=u^n_j$ *for* $t\in[t_n,t_{n+1})$ *and* $x\in C_j$, u^n_j *are defined by the scheme* (3.26), (2.12), *converges in* $L^p_{loc}([0,T]\times\mathbb{R}^N)$, *for all* $1\leqslant p<\infty$, *and all* $T>0$, *towards the unique entropy solution to* (1.1), (1.2) *as* $\Delta x\to 0$ *under* γ*-regularity requirement on mesh refinement process.*

Proof. Under suppositions of the theorem Propositions 3.1.1, 3.1.2, Lemma 3.3.1 are valid and the scheme (3.26), (2.12) can be interpreted as kinetic scheme. Then the convergence follows from the Theorem 4.2 of [8] where numerical scheme of the form (3.34) is studied. □

Remark 3.4. Some details on convergence of kinetic schemes in Ł$^\infty$ weak* compactness framework can be found in Appendix C.

4. Numerical test

In this subsection we present the results of our numerical investigation of these equilibrium type schemes (2.14). In all numerical tests given below the Engquist–Osher numerical flux function is used for discretization of space derivatives.

4.1. Test problems

We consider scalar conservation laws in two space dimensions with monomial flux functions and source terms:

$$\frac{\partial u}{\partial t}+\frac{\partial}{\partial x}\frac{u^\gamma}{\gamma}+\frac{\partial}{\partial y}\frac{u^\gamma}{\gamma}+z'_x(x,y)u^\beta+z'_y(x,y)u^\beta=0,\tag{4.1}$$

where β and γ are some positive constants and the function $z(x,y)$ is defined as

$$z(x,y) = \begin{cases} \cos(\pi(x+y)), & 4.5 \leqslant (x+y) \leqslant 5.5, \\ 0, & \text{otherwise.} \end{cases} \tag{4.2}$$

or

$$z(x,y) = \begin{cases} \sin(x^2+y^2-0.44), & x^2+y^2 < 0.44, \\ 0, & \text{otherwise,} \end{cases} \tag{4.3}$$

or

$$z(x,y) = \begin{cases} J \cdot \sin(2x+y), & x^2+y^2 < 0.44, \\ 0, & \text{otherwise,} \end{cases} \tag{4.4}$$

where J is a parameter. Clearly the later function is discontinuous and J defines the magnitude of the jump.

We supply Eq. (4.1) with different initial and boundary conditions thus obtaining a variety of test problems. In the four subsections below computational domain represents the square $\{0 \leqslant x \leqslant 5\sqrt{2}, 0 \leqslant y \leqslant 5\sqrt{2}\}$ and we use the following set of initial and boundary conditions:

$$\begin{aligned} u(0,x,y) &= \begin{cases} u_b, & 0 < x+y < 1, \quad 0 < x < 5\sqrt{2}, \quad 0 < y < 5\sqrt{2}, \\ 0, & 1 < x+y < 10, \quad 0 < x < 5\sqrt{2}, \quad 0 < y < 5\sqrt{2}; \end{cases} \\ \frac{\partial u}{\partial x} &= \frac{\partial u}{\partial y} \quad \text{on the border of the square.} \end{aligned} \tag{4.5}$$

Steady state solution of the problem (4.1), (4.5) is given by the following simple relation:

$$u(x,y) = \left(u_b^{\gamma-\beta} + (\gamma-\beta)(z(0,0) - z(x,y))\right)^{1/(\gamma-\beta)}. \tag{4.6}$$

In the last two subsections we start from a zero initial condition:

$$u(0,x,y) = 0, (x,y) \in \Omega, \quad \Omega \subset \mathbb{R}^2, \tag{4.7}$$

and we use the following Dirichlet boundary conditions

$$u(t,s) = u_b(s), \tag{4.8}$$

where s belongs to the border of the domain under consideration, i.e. $s \in \partial\Omega$ and u_b is a given L^∞ function.

4.2. Testing the scheme in one dimension

In this subsection we present the results of computations of the test problem with homogenous initial data in $x > 0$, Dirichlet boundary condition $u(t,0) = u_b$ and the function z defined by

$$z(x,y) = \begin{cases} (3-x)(7-x)\sin(\pi x), & 3 \leqslant x \leqslant 7, \\ 0, & \text{otherwise.} \end{cases}$$

The numerical results in Table 1 demonstrate that the equilibrium type scheme works in a stable and accurate way for different choices of γ and β, i.e., it is suitable for variety of equations.

Table 1
Equilibrium type schemes, one dimension, $u_b = 7.1$

Nodes	γ	β	CFL-number	L^∞-error	L^1-error
100	3	1	0.7	1.724×10^{-13}	5.31741×10^{-13}
100	3	2	0.7	2.55795×10^{-13}	9.64346×10^{-13}
100	4	1	0.7	1.45661×10^{-13}	6.60302×10^{-13}
100	4	2	0.7	1.7648×10^{-13}	7.45532×10^{-13}
100	4	3	0.7	6.49258×10^{-13}	2.37005×10^{-12}
100	5	1	0.7	2.0505×10^{-13}	9.51069×10^{-13}
100	5	3	0.7	2.44249×10^{-13}	1.04679×10^{-12}
100	4	3	0.7	1.46994×10^{-12}	5.39048×10^{-12}
100	6	1	0.7	2.62901×10^{-13}	3.09086×10^{-12}

4.3. Comparison with standard scheme

In Table 2(a) the numerical results are given for test problem (4.1), (4.5) with $u_b = 2, \gamma = 2, \beta = 1$ and the function z defined by (4.2). Uniform cartesian mesh is used in all computations presented in this subsection. In the second column of Table 2 the term "standard" stands for the scheme with standard cell centered discretization of source term, and the term "Equilibrium" corresponds to the scheme (2.14) given in Section 2.3.

Observe that by means of a change of variable we can reformulate the test problem (4.1), (4.5) as a one dimensional problem along the diagonal of the square. Notice also that 2-D schemes, both with standard and equilibrium type discretization of the source term, are equivalent to 1-D schemes on the lines parallel to the diagonal of the square. In order to avoid huge computations and obtain the results faster for Table 1 we have calculated corresponding 1-D problems, i.e., instead of 5001×5001 nodes we have used 10 001 nodes for equivalent scheme along the diagonal of the square, i.e., in one dimension. Pointing out from the results given in Table 2 we can conclude that our equilibrium type scheme is far more accurate than the standard one.

In Table 2(b) the results are given for the same test problem with $\gamma = 3$, $\beta = 1$. We compare four different schemes that differ from each other by different discretizations of source term only. Namely, we consider:

1. Standard scheme, i.e., scheme with cell centered discretization of source term.
2. Standard averaged scheme, i.e., the scheme that discretizes source term using some average of $b(u)$ at nodes of the stencil.
3. Standard upwind averaging, i.e., scheme that discretizes source term by means of using some average of $b(u)$ on an upwind stencil of Engquist–Osher numerical flux function. Notice that for the test prob-

Table 2
Comparison of numerical schemes, uniform rectangular mesh

Grid	Method	CFL-number	L^∞-error	L^1-error
(a)				
5001×5001	Standard	0.7	3.69×10^{-3}	5.56×10^{-3}
50×50	Standard	0.7	0.1650527	0.4880051
40×40	Equilibrium	0.7	1.5099×10^{-14}	7.13873×10^{-14}
(b) Eq. (4.1), $\gamma = 3$, $\beta = 1$, CFL = 0.7, time ≈ 50				
5001×5001	Standard		0.248537	0.32204
5001×5001	Standard averaged		0.2272184	0.301696
5001×5001	Standard upwind averaged		6.67489×10^{-3}	3.3734×10^{-2}
21×21	Equilibrium type		5.10703×10^{-15}	1.29148×10^{-14}

lem that we consider here derivatives of flux functions are always positive and therefore upwind stencil is fixed. Thus construction of the scheme is easy and in fact we do average $b(u)$ across edges of the upwind stencil. Observe also that some numerical schemes do use similar approaches for the upwind discretizaton of source terms, e.g., see the introduction.

4. Our equilibrium type scheme.

From Table 2(b) we conclude that averaging gives some advantage over standard cell centered discretization but errors are still big. Upwinding of source term improves accuracy significantly. Advantage of our equilibrium type scheme is evident: it produces much more accurate numerical solution than any other considered scheme and at the same time it uses several thousands times less nodal points compared to others. We will see in next subsections that equilibrium type scheme works in a stable and accurate way for equations containing more complex nonlinearities and in more complex geometries.

4.4. Studying the rate of convergence of the scheme

We use the same test problem as in previous subsection. We introduce two indicators characterizing the convergence of the scheme. The first one is the efficiency ratio defined as

$$\text{efficiency ratio} = \frac{\text{error for mesh } \mathscr{T}_1}{\text{error for mesh } \mathscr{T}_2}$$

assuming that a mesh $\mathscr{T}_2$ is more refined than a mesh $\mathscr{T}_1$.

The second one is the rate of the scheme defined as follows:

$$(\text{min. edge size})^{\text{rate}} = \text{error}. \tag{4.9}$$

Computations are performed with different numbers of nodes on finite volume mesh with a definition of a cell given in Fig. 6(a). The results are given in Tables 3 and 4, respectively for the equilibrium type and the standard scheme.

Observe that we do not reduce the size of the space step by a factor of two while passing from one line to the next one in Tables 3 and 4. Despite of this efficiency ratio is quite high for the equilibrium type scheme, while for the standard scheme it is close by 1, see Table 4. The most interesting feature we can observe from Table 3 is that the rate of the scheme increases together with mesh refinement that enables to conjecture that equilibrium type scheme might have the exponential convergence property, see Fig. 5(a), though formally it is first order accurate in space and in time in the sense of local truncation error. For the standard scheme the convergence rate is close to zero that ensures very slow convergence of this scheme. This can explain the fact that equilibrium type scheme ensures comparable with the standard one accuracy by means of 56712 times less nodal points, compare the line 2 in Table 3 and the line 1 in Table 2(a), see also Table 2(b). Another disadvantage of the standard scheme is that it produces large errors on the large domain, see Fig. 5(b) for the results along the diagonal of the square.

Table 3
Equilibrium type scheme, triangular mesh, CFL = 0.7

Nodes	Triangles	Min. edge	L^∞-error	Eff. ratio	Rate
121	200	0.1	1.475×10^{-2}	–	1.83
441	800	0.05	1.32×10^{-3}	11.17	2.21
961	1800	0.033	1.4×10^{-4}	9.43	2.61
1681	3200	0.025	2.0×10^{-5}	7	2.93
2601	5000	0.02	5.0×10^{-6}	4	3.12

Table 4
Standard scheme, triangular mesh, CFL = 0.7

Nodes	Triangles	Min. edge	L^∞-error	Eff. ratio	Rate
121	200	0.1	7.294×10^{-1}	—	0.137
441	800	0.05	4.134×10^{-1}	1.76	0.294
961	1800	0.033	3.377×10^{-1}	1.21	0.318
1681	3200	0.025	5.59×10^{-1}	0.6	0.15
2601	5000	0.02	5.51×10^{-1}	1.015	0.15

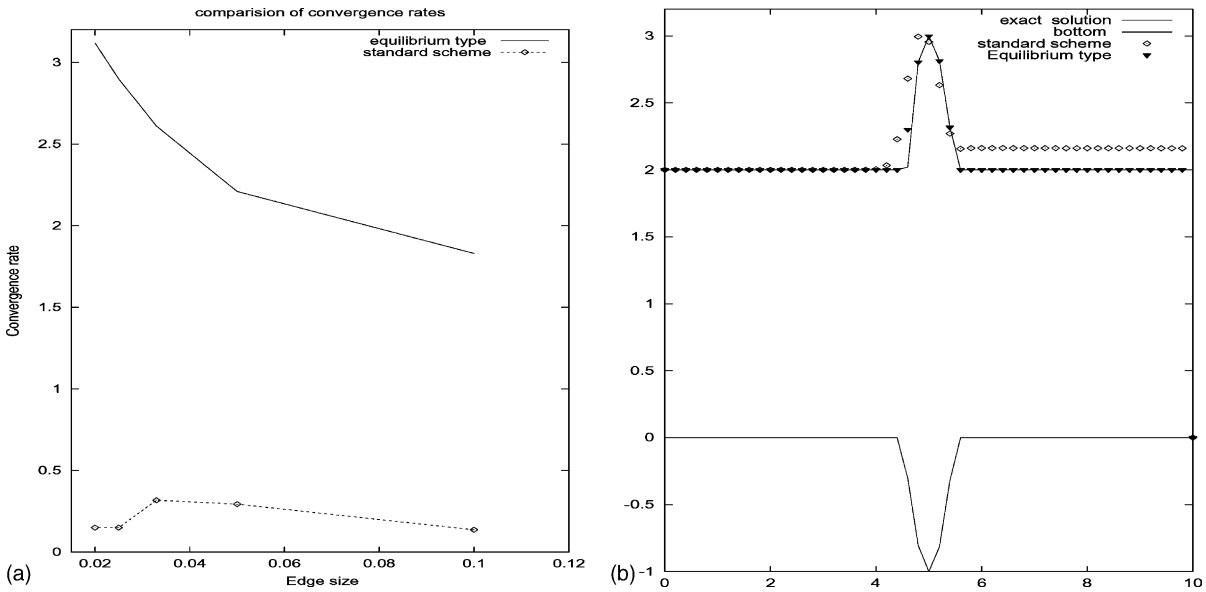

Fig. 5. Comparison of equilibrium type and standard schemes. (a) Convergence rates; (b) exact and approximate solutions.

Remark 4.1. Usually for the computation of the rate of the convergence of numerical schemes one uses the ratio of errors on nested meshes. If we use this approach to define convergence rate then for standard scheme we would have negative rate, see Table 4 lines 3 and 4. Notice that standard scheme is slowly convergent and a real convergence starts only late together with sufficiently large number of nodes. That is why we suppose that for the considered test problems formulae (4.9) is more suitable for the evaluation of the convergence rate. Observe also that convergence rate defined in this way is the same for two different meshes, see lines 4 and 5 in Table 4.

4.5. Studying the effect of a definition of a cell

Notice that for the same triangular mesh the cells of corresponding finite volume meshes can be defined in several different ways; e.g., for the same triangular mesh one can define median based cell as it was introduced in [1] or to define a cell by joining centers of gravity of the triangles surrounding the node as it was used in [3]. For the building the cells, we use the later approach but not necessarily with a true center of gravity of a triangle. From the γ regularity condition, see subsection 3.3.3 and [8], it seems plausible that cell definition should have some effect on the accuracy of computations since different cells give different re-

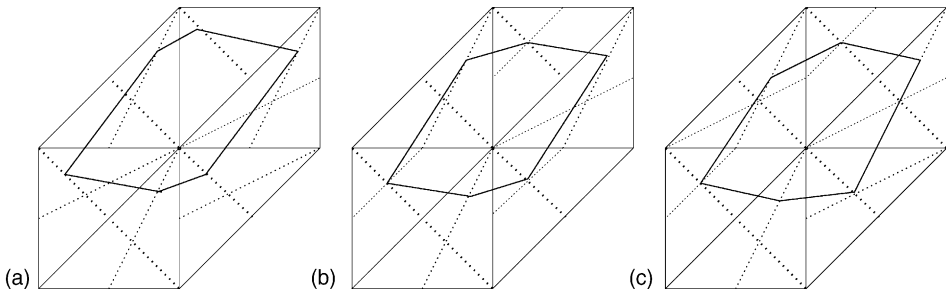

Fig. 6. Cells of finite volume meshes: (a) mesh 0; (b) mesh A; (c) mesh B.

Table 5
Triangular meshes: 1681 vertices, 3200 triangles, CFL = 0.7

Mesh No.	Standard	Equlibrium type
mesh0	0.51909	2×10^{-5}
meshA	0.47189	1×10^{-5}
meshB	0.47004	4×10^{-6}

Comparison of L^{∞}-errors on different finite volume meshes.

siduals. In order to investigate the problem numerically we have considered three different finite volume meshes. For *mesh*0 for all triangles the "center" is defined in the same way, as an average of the vertices of the triangle with coefficients 1/6, 1/6, 2/3, see Fig. 6(a). For *meshA* the "center" is defined in the same way for couples of triangles. For the first triangle the "center" is the same as in previous case and for the second one it is average of vertices of the triangle with coefficients 1/4, 1/4 1/2. example of corresponding cell is given on Fig. 6(b); For *meshB* the "center" is defined in the same way for triples of triangles. For the first two triangle the "center" is defined in the same way as in case of the *meshA* and for the third one the center is the intersection of medians. Example of one of the possible cells for *meshB* is given in Fig. 6(c); Numerical results of the same test problem as in previous subsection are given in Table 5. These results given in Table 5 indicate that different cell definition affects the precision of both, standard and equilibrium type, numerical schemes. Pointing out from these results we can conjecture that accuracy of computations increases with the regularity of finite volume mesh, e.g., compare the cells given in Fig. 6. We can also conclude that equilibrium type scheme has high precision for any type of considered above cells.

4.6. Numerical model of boundary conditions. Testing the scheme in curvilinear geometry

In this subsection we introduce a numerical method for the treatment of Dirichlet boundary condition for scalar conservation laws, see (4.8). Recall that boundary conditions for scalar conservation laws have been introduced by Bardos et al. [4] via vanishing viscosity method. This approach enables to treat (4.8) in a suitable way ensuring consistency with the entropy condition thus taking into account characteristic directions. Consult [20] and references there in for various treatment of boundary conditions for hyperbolic conservation laws at continuous and discrete levels. Here we propose one simple and useful numerical model of boundary conditions. Notice that for bounded domains first we should precise further the definition of finite volume cells since for the nodes on the border it is impossible to apply the rule given above in Section 4.5. The finite volume cells comprising nodal points on a border of a domain under consideration

are called boundary cells. Suppose a triangulation of a bounded domain Ω is given and Γ is a border of this domain. Then we can define boundary cells by means of the following procedure:

(i) joining midpoints of neighbor triangles comprising boundary node as a vertex; (ii) joining midpoint of boundary edge to the boundary node and to the center of the triangle comprising boundary edge.

Observe that with this definition parts of a border are considered as "interfaces" of boundary cells. Now the problem is to define numerical solution in the nodes on the border. Notice that due to hyperbolicity of the scalar conservation laws, in general, in nodal points of the border we can not update approximate solution by means of trivial treatment of Dirichlet boundary condition (4.8). That is why we introduce numerical model of boundary condition that consists of the following three steps:

(i) extrapolate Dirichlet boundary data outside of domain, i.e., we set $u = u_b$ in the vicinity of a border;

(ii) compute some averaged approximated solution in the boundary cell, i.e., if $\vec{x_j}$ is nodal point on the border we compute:

$$\frac{v_j^{n+1} - u_j^n}{\Delta t} + \sum_{k, l\Gamma_{jk}^l \cap \Gamma = \emptyset} \frac{|\Gamma_{jk}^l|}{|C_j|} A(u_j^n, u_k^n, \vec{n}_{jk}^l) + \sum_{k, l\Gamma_{jk}^l \cap \Gamma \neq \emptyset} \frac{|\Gamma_{jk}^l|}{|C_j|} A(u_j^n, u_{bj}^n, \vec{n}_{jk}^l) = 0, \tag{4.10}$$

where u_{bj}^n is boundary data computed in node $\vec{x_j}$ at $t = t_n$.

(iii) Extrapolate this computed averaged value into the node on the border, i.e., we set $u_j^{n+1} = v_j^{n+1}$.

In order to test the developed equilibrium type scheme on domains with curvilinear geometry we couple the scheme with the above numerical model of boundary conditions. We consider the test problem (4.1), (4.7), (4.8), where $\gamma = 2, \beta = 1$ and the prescribed boundary value function is constant. Namely, we set $u_b = 2$. Then clearly exact steady state solution of initial boundary value problem (4.1), (4.7), (4.8) can be determined again by formulae (4.6). For this test problem we consider two different computational domains Ω. One computational domain is an unit circle; boundary curve of another computational domain in parametric form writes:

$$t \in (0, 2 \cdot \Pi); x(t) = (0.65 + \sin(2.5 \cdot t)^2) \cdot \cos(t), y(t) = \sin(t).$$

Computation of the test problems are performed on three different triangular meshes, see Fig. 7, with CFL-number 0.75. Each refined mesh contains double number of boundary nodes compared to precedent rough triangulation, namely we have used 25, 50 and 100 boundary nodes. The function $z(x, y)$ presented in the source term of Eq. (4.1) is given in Fig. 8. Numerical results of computations of these two test problems are given in Figs. 10–12. Namely, see Figs. 10 and 11 for convergence history on fine meshes and see Fig. 12 for the streamlines of the error function defined as $(u_{\text{numer}} - u_{\text{exact}}) \times F$ on three different meshes. The factor F is different for different meshes, namely $F = 10^4, 10^4, 10^{12}$ for left and $F = 10^3, 10^3, 10^4$ for right figure respectively. We can observe that together with mesh refinement the errors decrease in the magnitude and subdomains where errors are presented narrow substantially. Notice also that the complexity of the geometry affects the accuracy: the results are less accurate in more complex geometry. The latter can be also ensured by the irregularity of the triangulation, see Fig. 7 right. More numerical results for Eqs. (4.1), (4.3), (4.7), (4.8), $u_b = 2$, for different α and γ are given in Table 6. We can conclude that the equilibrium type scheme in conjunction with the above numerical model of boundary condition produces quite accurate numerical solutions.

4.7. Studying the convergence of time marching procedure

We consider the same test problem as in previous subsection. Computational domain is unit circle with triangulation corresponding to 50 boundary nodes, see Fig. 7. Computations for equilibrium type scheme are performed for time interval $(0, 5)$, for the standard scheme computations are done for time interval

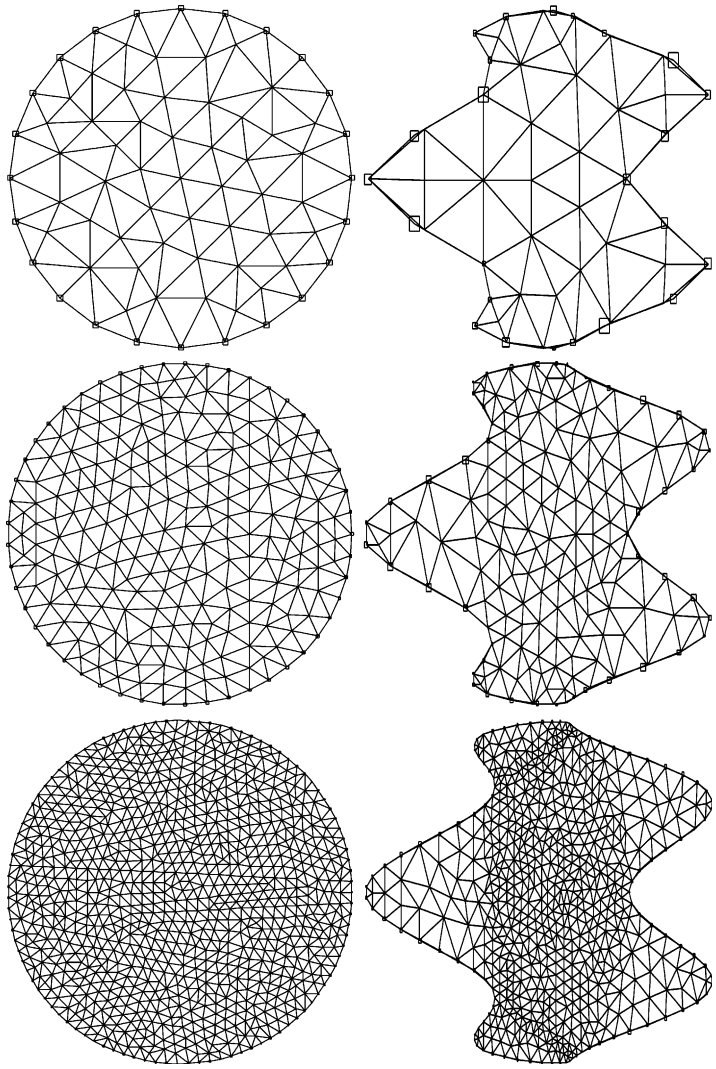

Fig. 7. Computational domains and triangular meshes.

$(0, 100)$. For some selected time moments the errors in L^∞ and L^1 norms are given in Tables 7 and 8 for standard and equilibrium type schemes respectively.

The advantage of equilibrium type scheme is evident. For $t = 3.2$ it produces accurate numerical solution; namely the accuracy is of order 10^{-13} in L^∞ and L^1 norms and this precision is maintained exactly in further computations, i.e., $||u^{n+1} - u^n|| = 0$ when $t_n \geqslant 3.2$. The standard scheme produces most accurate solution at $t \approx 17$. Then for $t \approx 42$ the scheme converges to its steady state that is maintained exactly for $t_n > 42$. Observe that steady state of the standard scheme differ very much from the exact steady state solution of the governing equation, e.g., see Table 7 for the errors.

Notice that equilibrium type scheme is consistent with unsteady equation. From the considered test problem and computational results given in Table 8 we can conjecture that for $t = 3$ exact solution of our test problem coincides with steady state solution. But for $t = 3$ the errors of standard scheme are over 1.

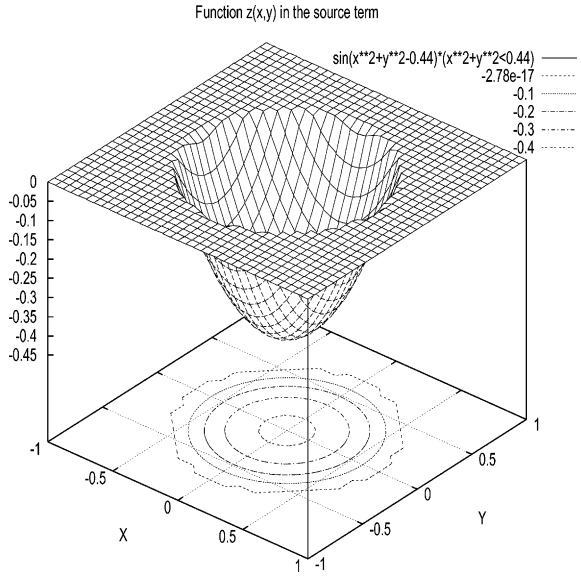

Fig. 8. Continuous function $z(x, y)$.

Table 6
Eq. (4.1), time ≈ 2.5, L^∞-error, CFL $= 0.75$, mesh with 50 boundary nodes

α	β	Fig. 7 left	Fig. 7 right
3	1	4.92712×10^{-13}	1.67636×10^{-13}
3	2	2.36696×10^{-13}	4.7163×10^{-13}
4	1	2.10715×10^{-13}	5.12034×10^{-13}
4	2	1.98059×10^{-13}	1.23455×10^{-13}
4	3	2.96203×10^{-13}	6.22389×10^{-13}

Table 7
Convergence of time marching procedure, standard scheme, CFL $= 0.75$

Time	L^∞-error	L^1-error
2	1.4717	2.9347
3	1.2074	2.2197
5	0.8905	1.359
9	0.4914	0.53103
17	0.1511	0.1249
32	0.15502	0.1335
>42	0.15507	0.13357

Thus we can conclude that standard scheme is also not suitable for calculation of nonstationary problems because it produces highly erroneous approximate solution.

4.8. Studying dependence on CFL number

Notice that CFL condition dictated by Lemma 3.1.1 is too restrictive. That is why in all computations we use the usual CFL condition for homogenous equation. We conjecture that this standard CFL condition

Table 8
Convergence of time marching procedure, equilibrium type scheme, CFL = 0.75

Time	L^∞-error	L^1-error
1.16	1.5939	0.1635
1.47	9.3109×10^{-3}	1.1663×10^{-3}
1.94	6.3418×10^{-6}	1.0936×10^{-6}
2.25	4.3038×10^{-7}	8.8194×10^{-9}
2.57	5.3965×10^{-10}	1.1876×10^{-10}
2.88	9.0514×10^{-12}	1.5963×10^{-12}
>3.2	2.4691×10^{-13}	1.7305×10^{-13}

Table 9
Standard scheme, dependence of L^∞-error on CFL-number

CFL	time ≈ 3	time ≈ 42
0.1	1.2081	0.15507
0.4	1.2078	0.15507
0.75	1.2074	0.15507
0.9	1.2075	0.15507

Table 10
Equilibrium type scheme, dependence of L^∞-error on CFL-number

CFL	time ≈ 1.94	time ≈ 3.2
0.1	7.2338×10^{-6}	1.5949×10^{-12}
0.4	7.0913×10^{-6}	4.281×10^{-13}
0.75	6.3418×10^{-6}	2.4691×10^{-13}
0.9	6.0478×10^{-6}	2.0696×10^{-13}

produces time steps that are small enough to be suitable for computation of a contribution of a source for a single time step. Then using the same CFL condition for the calculation of the next time step does already take into account the contributions of a source done at previous time level. In order to check the conjecture we study influence of various CFL numbers on accuracy of computations. The L^∞-errors in two different time moments are given in Tables 9 and 10 for standard and equilibrium type schemes respectively. From these results we can conclude that smaller CFL numbers do not give any advantage. Thus for the scalar conservation laws with source term using of the standard CFL condition is acceptable.

4.9. Dirac mass in the source

When the function z is discontinuous then, clearly, Dirac mass appears in the source of Eq. (1.1). This is the case with the function z defined by (4.4), see Fig. 9. Then Dirac mass is concentrated on the circle defined by $x^2 + y^2 = 0.44$, i.e.the source tends to infinity on the above circle. In this subsection we consider test problem (4.1), (4.7), (4.8), where $\Omega = \textit{unit circle}$, $\gamma = 2$, $\beta = 1$, $u_b = 2$. Also we consider various values of the parameter J that controls the magnitude of jump in the discontinuity of the function $z(x, y)$. Computations are performed for three different triangulations, see Fig. 7 left. The equilibrium type scheme for these test problems produces accurate solutions: see Table 11 for errors computed for different values of J, see Fig. 13 for the convergence history on fine mesh and see Table 12 for mesh refinement history. Notice also that equilibrium type scheme gives good results for test problem with $\beta = 2$, while standard scheme with cell centered discretization of the source is unstable.

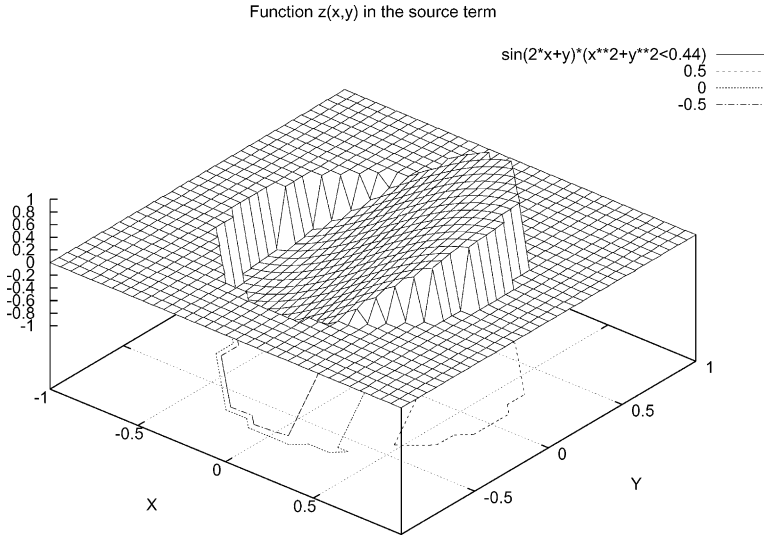

Fig. 9. Discontinuous function $z(x, y)$.

Table 11
Jumps in the source, rough mesh = 25 boundary nodes, CFL = 0.5, time ≈ 7.0001, L^∞-errors

Jump	1	2	3	4	5	6	7
Error	1.135×10^{-13}	4.383×10^{-13}	2.485×10^{-6}	2.047×10^{-6}	1.427×10^{-7}	6.055×10^{-8}	1.057×10^{-7}

Table 12
Mesh refinement history; discontinuous source term, $J = 1$, CFL = 0.75

Time	Nodes on border	L^∞-error
2.50018	25	3.30241×10^{-3}
2.50009	50	2.91488×10^{-6}
2.50008	100	1.43396×10^{-8}

5. Equilibrium type schemes for systems of conservation laws

In this subsection we present a formal extension of equilibrium type schemes for systems of conservation laws. For the simplicity we consider the following system in one space dimension only:

$$\frac{\partial \vec{u}}{\partial t} + \frac{\partial \vec{A}(\vec{u})}{\partial x} + B(\vec{u}) \frac{\partial \vec{z}(x)}{\partial x} = 0, \quad t \geqslant 0, \ \ x \in \mathbb{R}, \tag{5.1}$$

where $\vec{u}$ is m-dimensional vector, $\vec{A}(\vec{u})$ and $\vec{z}(x)$ are m-dimensional vector functions, $B(\vec{u})$ is $m \times m$ matrix. We assume that corresponding to (5.1) steady state equation

$$\frac{\partial \vec{A}(\vec{u})}{\partial x} + B(\vec{u}) \frac{\partial \vec{z}(x)}{\partial x} = 0, \tag{5.2}$$

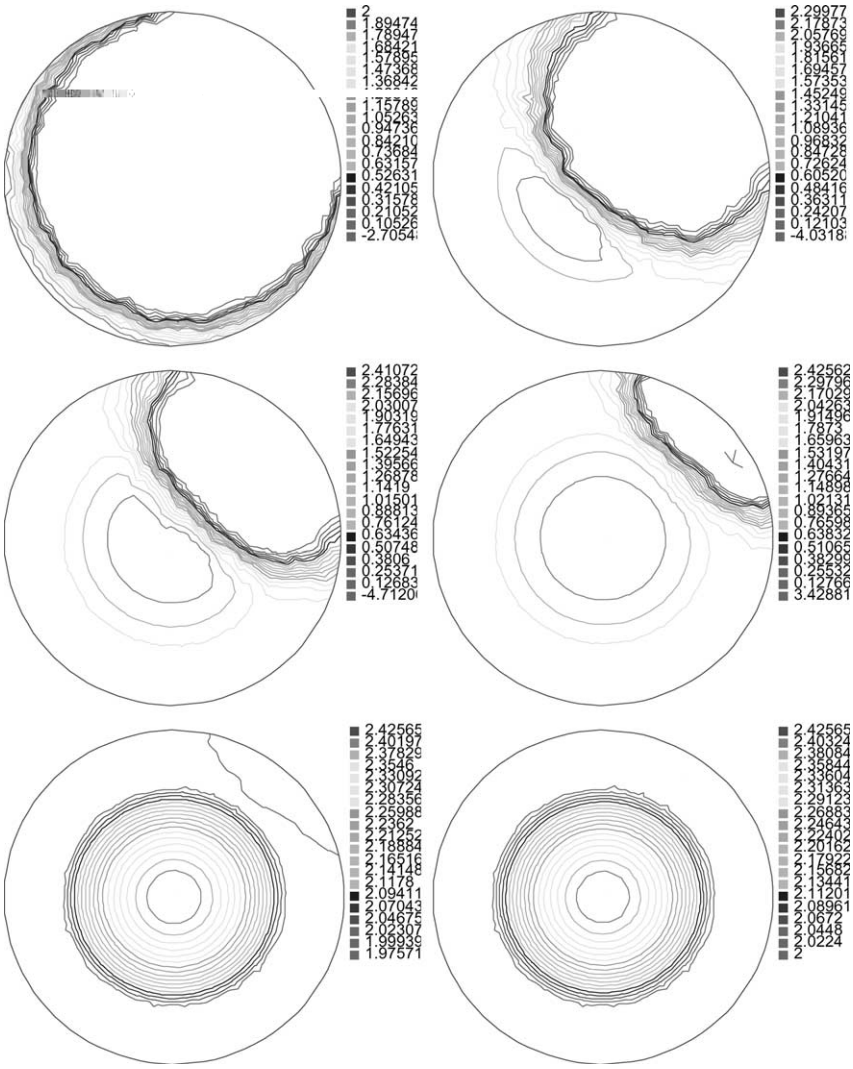

Fig. 10. Continuous source term. Initial-boundary value problem. Convergence history.

can be equivalently written as

$$\frac{\partial \vec{D}(\vec{u})}{\partial x} + \frac{\partial \vec{z}(x)}{\partial x} = 0, \tag{5.3}$$

where $\vec{D}(\vec{u})$ is some vector function, referred onward as steady state flux function. We assume also that $[\nabla \vec{D}]^{-1}$ exists. In order to apply the algorithm described in Section 2 some analogy of formulae (2.1) is needed. (5.2) and (5.3) equivalently can be written as follows:

$$\nabla \vec{A}(\vec{u}) \frac{\partial \vec{u}}{\partial x} + B(\vec{u}) \frac{\partial \vec{z}(x)}{\partial x} = 0, \tag{5.4}$$

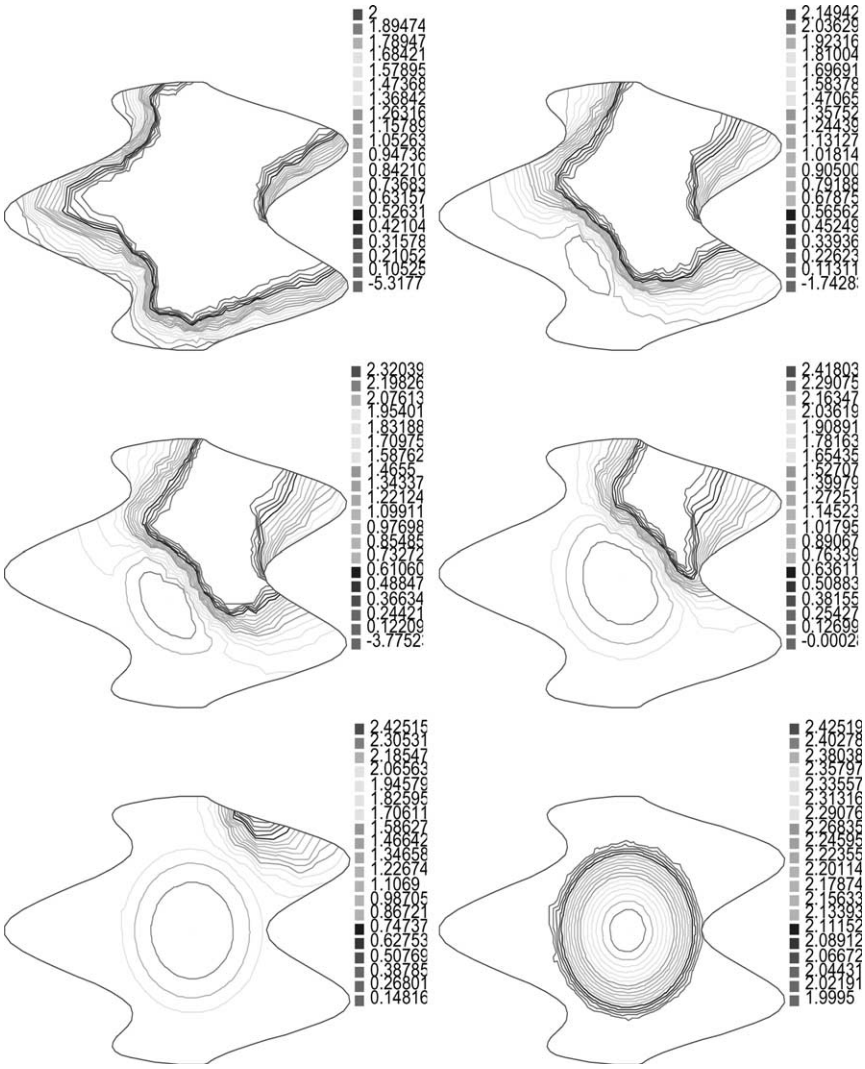

Fig. 11. Continuous source term. Initial-boundary value problem. Convergence history.

$$\nabla \vec{D}(\vec{u}) \frac{\partial \vec{u}}{\partial x} + \frac{\partial \vec{z}(x)}{\partial x} = 0. \tag{5.5}$$

From (5.4) and (5.5) we easily derive the desired representation of matrix $B(\vec{u})$,

$$B(\vec{u}) = \nabla \vec{A}(\vec{u}) \cdot [\nabla \vec{D}]^{-1}. \tag{5.6}$$

Using (5.6) and following the algorithm given in Section 2 we propose the analogy of the scheme (2.8):

$$\frac{\vec{u}_j^{n+1} - \vec{u}_j^n}{\Delta t} + \frac{\vec{A}(\vec{u}_{j+1}^n, \vec{u}_j^n) - \vec{A}(\vec{u}_j^n, \vec{u}_{j-1}^n)}{\Delta x} + \nabla \vec{A}(\vec{u}_{j+1}^n, \vec{u}_j^n, \vec{u}_{j-1}^n) \cdot [\nabla \vec{D}(\vec{u}_{j+1}^n, \vec{u}_{j-1}^n)]^{-1} \cdot \frac{\vec{z}_{j+1} - \vec{z}_{j-1}}{\Delta x} = 0, \tag{5.7}$$

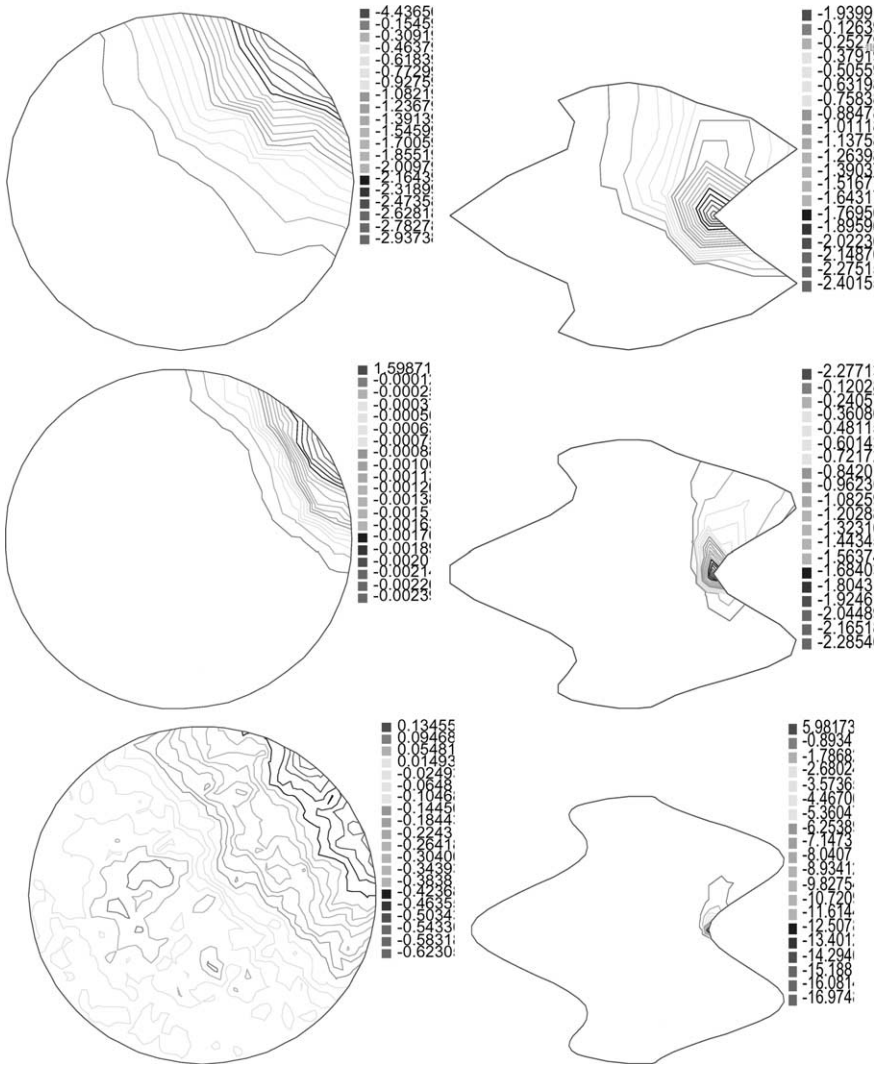

Fig. 12. Continuous source term. Streamlines of $(u_{\text{numer}} - u_{\text{exact}}) \times F$ on three different meshes; $F = 10^4$, 10^4, 10^{12} for left and $F = 10^3$, 10^3, 10^4 for right figure respectively.

where the elements of matrixes $\nabla\vec{A}(\vec{u}^n_{j+1}, \vec{u}^n_j, \vec{u}^n_{j-1})$ and $\nabla\vec{D}(\vec{u}^n_{j+1}, \vec{u}^n_{j-1})$ are defined according to the following formulae:

$$a_{kl}(\vec{u}^n_{j+1}, \vec{u}^n_j, \vec{u}^n_{j-1}) = \frac{\vec{A}_k(\vec{u}^n_{j+1}, \vec{u}^n_j) - \vec{A}_k(\vec{u}^n_j, \vec{u}^n_{j-1})}{\vec{u}^n_{l,j+1} - \vec{u}^n_{l,j-1}},$$

$$d_{kl}(\vec{u}^n_{j+1}, \vec{u}^n_j, \vec{u}^n_{j-1}) = \frac{\vec{D}_k(\vec{u}^n_{j+1}, \vec{u}^n_j) - \vec{D}_k(\vec{u}^n_j, \vec{u}^n_{j-1})}{\vec{u}^n_{l,j+1} - \vec{u}^n_{l,j-1}}.$$

The subscripts k, l in the left-hand sides of the above formulae refer to the components of matrixes, in the right-hand sides the subscript l refers to the elements of the vector. Observe that

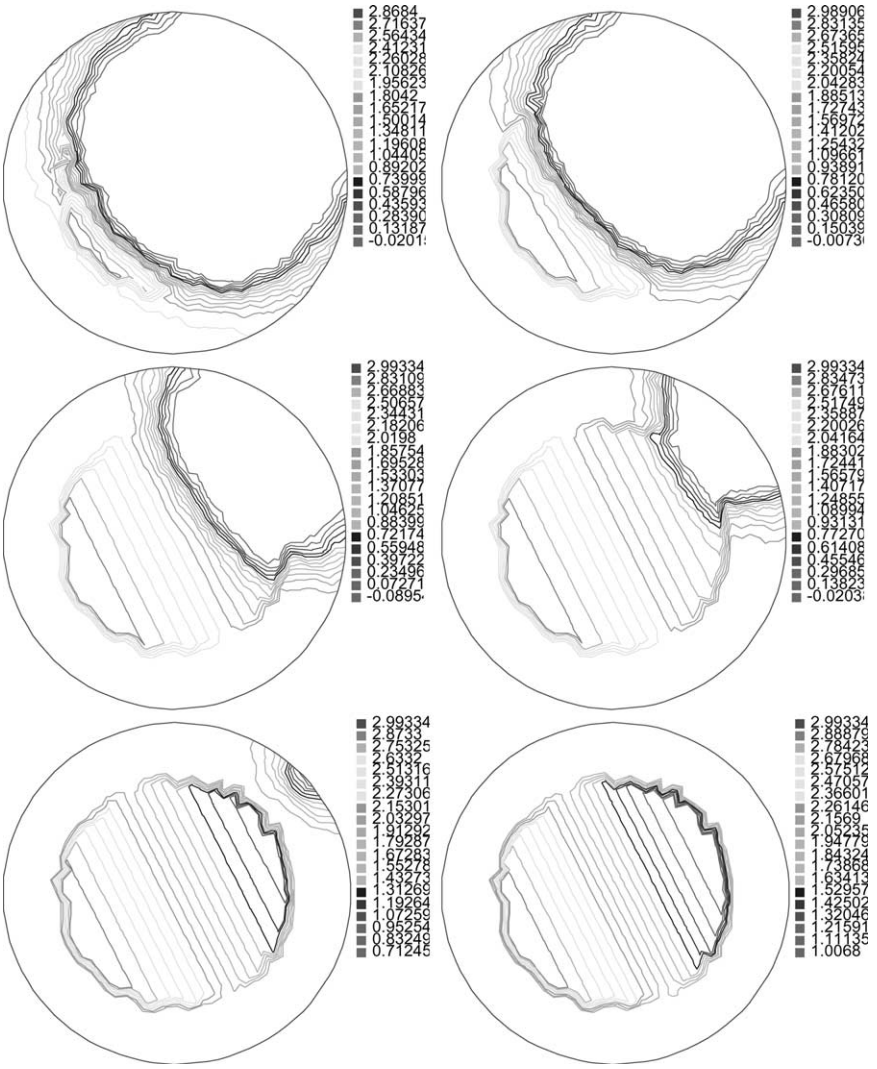

Fig. 13. Discontinuous source term. Initial-boundary value problem. Convergence history.

$$\nabla\vec{A}(\vec{u}^n_{j+1},\vec{u}^n_j,\vec{u}^n_{j-1})\cdot(\vec{u}^n_{j+1}-\vec{u}^n_{j+1})=\vec{A}(\vec{u}^n_{j+1},\vec{u}^n_j)-\vec{A}(\vec{u}^n_j,\vec{u}^n_{j-1}), \tag{5.8}$$

$$\nabla\vec{D}(\vec{u}^n_{j+1},\vec{u}^n_{j-1})\cdot(\vec{u}^n_{j+1}-\vec{u}^n_{j+1})=\vec{D}(\vec{u}^n_{j+1})-\vec{D}(\vec{u}^n_{j-1}). \tag{5.9}$$

Proposition 5.0.1. *Finite volume scheme* (2.14) *is exact on the equilibrium states of hyperbolic conservation laws* (5.1).

Proof. Observe that equilibria of Eq. (5.1) are defined by Eq. (5.1) integration of which yields the following relation:

$$\vec{D}(\vec{u}^n_{j+1}) - \vec{D}(\vec{u}^n_{j-1}) = -(\vec{z}^n_{j+1} - \vec{z}_{j-1}). \tag{5.10}$$

Suppose initial data are at equilibrium. Then with account of (5.10), (5.9) we have:

$$\begin{aligned}
&\nabla\vec{A}(\vec{u}^n_{j+1}, \vec{u}^n_j, \vec{u}^n_{j-1}) \cdot [\nabla\vec{D}(\vec{u}^n_{j+1}, \vec{u}^n_{j-1})]^{-1} \cdot (\vec{z}_{j+1} - \vec{z}_{j-1}) \\
&\quad = -\nabla\vec{A}(\vec{u}^n_{j+1}, \vec{u}^n_j, \vec{u}^n_{j-1}) \cdot [\nabla\vec{D}(\vec{u}^n_{j+1}, \vec{u}^n_{j-1})]^{-1} \cdot (\vec{D}(\vec{u}^n_{j+1}) - \vec{D}(\vec{u}^n_{j-1})) \\
&\quad = -\nabla\vec{A}(\vec{u}^n_{j+1}, \vec{u}^n_j, \vec{u}^n_{j-1}) \cdot [\nabla\vec{D}(\vec{u}^n_{j+1}, \vec{u}^n_{j-1})]^{-1} \cdot \nabla\vec{D}(\vec{u}^n_{j+1}, \vec{u}^n_{j-1}) \cdot (\vec{u}^n_{j+1} - \vec{u}^n_{j-1}) \\
&\quad = -\nabla\vec{A}(\vec{u}^n_{j+1}, \vec{u}^n_j, \vec{u}^n_{j-1}) \cdot (\vec{u}^n_{j+1} - \vec{u}^n_{j-1}) = -(\vec{A}(\vec{u}^n_{j+1}, \vec{u}^n_j) - \vec{A}(\vec{u}^n_j, \vec{u}^n_{j-1})).
\end{aligned}$$

Substituting approximation of source term with the latter expression in numerical scheme (5.7) yields:

$$\frac{\vec{u}^{n+1}_j - \vec{u}^n_j}{\Delta t} = 0,$$

i.e., equilibrium initial data are maintained. □

Remark 5.1. Extension of the scheme to several space dimensions can be done exactly in the same way as for the scalar equation in Section 2.4. In particular for the discretization of source term at cell interfaces we can apply one dimensional algorithm in directions across/perpendicular to cell interfaces.

Remark 5.2. The presented algorithm is valid in the range of the validity of formula (5.6). Standard discretization of the source with suitably selected weight can be applied for cell interfaces where $\nabla\vec{D}$ is degenerated. For some systems this approach can still capture all the equilibria exactly, as in the scalar case, but not in general. Thus some adjustment of the presented algorithm can be needed for concrete problems.

Appendix A. Proof of Lemma 1.0.1

Proof. Notice that $x_j, x_k \in \Omega$, Ω is open and connected. In Ω there exist some continuous curve γ connecting x_j and x_k. Denote d the distance between γ and $\partial\Omega$. Let r any positive number such that $r < d$. Denote $P_{N-1}(x, \vec{n})$ $N-1$ dimensional plane in $\mathbb{R}^N$ such that $x \in P_{N-1}(x, \vec{n})$ and $\vec{n} \perp P_{N-1}(x, \vec{n})$. Denote p points on these $N-1$ dimensional planes. For every point $x \in \gamma$ we call $B_r(x)$, $B_r(x) \subset P_{N-1}(x, \vec{n})$, $N-1$ dimensional ball of radius r and center x. Let C_r be "curvilinear cylinder", $C_r = \bigcup_{x\in\gamma} B_r(x)$. Under third supposition of the lemma and from (1.11) over the cylinder C_r we have:

$$\int_{B_r(x_j)} \langle D(u(p_j) + z(p_j), \vec{n}\rangle dp_j - \int_{B_r(x_k)} \langle D(u(p_k) + z(p_k), \vec{n}\rangle dp_k = 0.$$

Suppose L linear transformation, $L : B_r(x_j) \to B_r(x_k)$. With account of this the latter equation equivalently writes:

$$\int_{B_r(x_k)} \big(\langle D(u(L(p_k)) + z(L(p_k)), \vec{n}\rangle |L| - \langle D(u(p_k) + z(p_k), \vec{n}\rangle\big) dp_k = 0.$$

Observe that according to our construction $r < d$, r is arbitrary positive number and under supposition of the lemma the function under integral is continuous. Then the latter equation yields that the function under integral is zero in x_k, i.e., (1.12) is satisfied. □

Appendix B. Uniqueness of generalized kinetic solutions

Theorem B.0.1 (Uniqueness of generalized kinetic solutions [7]). *Let* $f(t,x,\xi$

$$\Psi_{i,\Delta x}(t) \to \Psi_i(t) \text{ in } L^\infty - w*, \quad \Psi_i(t) \text{ is continuous and } \Psi_i(0) = 0. \tag{C.19}$$

Then, as $\Delta x \to 0$, $u_{\Delta x}$ *converges strongly in* $L^p([0,T] \times \mathbb{R}^N)$, $1 \leqslant p < \infty$, *to the unique entropy solution to* (1.1), (1.2).

Notice that the requirements of the main convergence theorem represent suitable approximations of the conditions of the uniqueness theorem of generalized kinetic solutions, e.g., (C.13), (C.14) represent the analogy of the kinetic Eq. (3.19); (C.15) ensures validity of the entropy inequality; (C.16) together with (C.13) ensure consistency of the approximate solution with (3.19), (3.20); (C.17), (C.18) are approximations of (B.11) and (B.12), respectively.

In order to prove the convergence of numerical schemes it is sufficient to verify that the scheme satisfies the assumptions of the Abstract Convergence Theorem.

Appendix D. On verification of requirements of the abstract convergence theorem

Here we just briefly recall some important steps on application of the abstract convergence theorem under suppositions of the Theorem 3.3.2 for Eq. (3.34).

(1) First the case of the compactly supported initial function $u_0(x)$ is considered. Then general case can be treated by means of the so-called standard diagonalization process of approximate solutions corresponding to different compactly supported data, see e.g., [7].

(2) Verification of (C.16). L^∞ bound is controlled by Proposition 3.1.1. Because of the compactly supported initial value function, (1.3) and finite speed of propagation of perturbations, uniform L^∞ bound ensures uniform L^1 estimate.

(3) Verification of (C.13), (C.14). According to Lemma 3.3.1 numerical scheme (3.34) can be equivalently written in a suitable form that accepts kinetic interpretation, see Remark 3.3. Notice that (C.13), (C.14) are considered in a weak sense. For the derivation of (C.13) the standard technique is to multiply kinetic scheme on $\varphi_j^n(\xi) = \varphi(t_n, x_j, \xi)$, $\varphi(t,x,\xi)$ is some test function, and then to apply integration by parts formulae at a discrete level. In order to ensure (C.14) in several space dimensions we have additional requirement on regularity of mesh refinement process. Estimation of $\Psi_{\Delta x}$ is given in details in [8].

(4) Derivation of (C.15). If nonnegativity of the measure $m_{\Delta x}$ is known then its bound is easily recovered just by means of integration of the discrete kinetic equation. In [7] verification of the nonnegativity of the measure is based on Brenier's lemma [10]. For the case under consideration application of this technique is not possible and in cell entropy inequality is needed at macroscopic level. Notice that such entropy inequality is provided by Proposition 3.1.2. Then details can be found in [8].

(5) Derivation of (C.17)–(C.19). After step 2 this is trivial since application of the similar technique is sufficient. Details can be found in [7].

References

[1] F. Angrand, A. Dervieux, V. Boulard, J. Periaux, G. Vijayasundaram, Transonic Euler simulation by means of finite element explicit schemes, AIAA-83, 1984.

[2] C. Arvatis, T. Katsaunis, C. Makridakis, Adaptive finite element relaxation schemes for hyperbolic conservation laws, Math. Model. Numer. Anal. 35 (1) (2000) 17–33.

[3] E. Audusse, M.-O. Bristeau, B. Perthame, Kinetic schemes for Saint–Venant equations with source termes on unstructured grids, INRIA Report, RR 3989, 2000.

[4] C. Bardos, A. LeRoux, J. Nedelec, First order quasilinear equations with boundary conditions, Commun. Partial Diff. Equat. 4 (1979) 1017–1034.

[5] A. Bermudez, A. Dervieux, J.-A. Desideri, M.E. Vazquez, Upwind schemes for two-dimensional shallow water equations with variable depth using unstructured meshes, Comput. Meth. Appl. Mech. Eng. 155 (1998) 49–72.

[6] A. Bermudez, M.E. Vazquez, Upwind methods for hyperbolic conservation laws with source terms, Comput. Fluids 23 (8) (1994) 1049–1071.
[7] R. Botchorishvili, B. Perthame, A. Vasseur, Equilibrium schemes for scalar conservation laws with stiff sources, Math. Comput. 72 (2003) 131–157.
[8] R. Botchorishvili, Equilibrium type schemes for multidimensional in space scalar conservation laws with source term, Appl. Math. Inform. 6 (2) (2002).
[9] R. Botchorishvili, Implicit kinetic schemes for scalar conservation laws, Numer. Meth. Part. Diff. Equat. 18 (1) (2002) 26–43.
[10] Y. Brenier, Résolution d'équations d'évolution quasilinéaires en dimensions N d'espace à l'aide d'équations linéaires en dimensions N+1, J. Diff. Equat. 50 (3) (1982) 375–390.
[11] M.O. Bristeau, B. Perthame, Transport of pollutant in shallow water using kinetic schemes, ESAIM-Proceedings 10 (CEMRACS) (1999) 9–21.
[12] C. Chainais, L. Hillairet, First and second order schemes for a hyperbolic equation: convergence and rate estimate, in: F. Benkhaldoun, R. Vilsmaier (Eds.), Finite Volumes for Complex Applications; Problems and Perspectives, Hermes Paris, 1997, pp. 137–144.
[13] B. Cockburn, F. Coquel, P. LeFloch, An error estimate for finite volume multidimensional conservation laws, Techical Report 285, CMAPX, Ecole Politechnique, 1993.
[14] F. Coquel, P. LeFloch, Convergence of finite difference schemes for conservation laws in several space dimensions: the corrected antidiffusive flux approach, Math. Comput. 57 (1991) 169–210.
[15] R. Eimard, T. Galouet, R. Herbin, Finite volume methods, in: P.G. Ciarlet, J.-L. Lions (Eds.), Handbook of Numerical analysis, Vol. VIII, Solutions of equations in R_n. Part 4. Techniques of scientific computing. Part 4. Numerical methods for fluids. Part 2. North-Holland, Amsterdam, 2002.
[16] B. Depres, F. Lagoutiere, Generalized Harten's formalism and longitudinal variation diminishing schemes for linear advection on arbitrary grids, LAN Report 0045, Universite Pierre et Marie Curie, 2000.
[17] R.J. DiPerna, Measure valued solutions to conservation laws, Arch. Rat. Mech. Anal. 88 (1985) 223–270.
[18] B. Engquist, S. Osher, Stable and entropy satisfying approximations for transonic flow calculations, Math. Comput. 34 (1980) 45–75.
[19] L. Gascon, J.M. Corberan, Construction of second-order TVD schemes for nonhomogenous hyperbolic conservation laws, J. Comput. Phys. 172 (2001) 261–297.
[20] E. Godlewski, P.A. Raviart, Numerical approximations of hyperbolic systems of conservation laws, Applied Mathematics Science, vol. 118, Springer, New York, 1996.
[21] L. Gosse, A.-Y. Leroux, A well-balanced scheme designed for inhomogeneous scalar conservation laws, C. R. Acad. Sc., Paris Sér. I 323 (1996) 543–546.
[22] L. Gosse, A well-balanced scheme using non-conservative products designed for systems of conservation laws with source terms, Comput. Math. Appl. 39 (2000) 135–159.
[23] J.M. Greenberg, A.-Y. LeRoux, A well balanced scheme for numerical processing of source terms in hyperbolic equations, SIAM J. Numer. Anal. 33 (1996) 1–16.
[24] J.M. Greenberg, A.-Y. LeRoux, R. Baraille, A. Noussair, Analysis and approximation of conservation laws with source terms, SIAM J. Numer. Anal. 34 (5) (1997) 1980–2007.
[25] S. Jin, A steady-state capturing method for hyperbolic systems with geometrical source terms, Math. Model. Num. Anal. 35 (2001) 631–645.
[26] P. Jenny, B. Miller, Rankine–Hugoniot–Riemann solver considering source terms and multidimensional effects, J. Comput. Phys. 145 (1998) 575–610.
[27] S.N. Kruzkov, Generalized solutions of the Cauchy problem in the large for nonlinear equations of first order, Dokl. Akad. Nauk. SSSR 187 (1) (1970) 29–32, English trans, Soviet Math. Dokl. 10 (1969).
[28] N.N. Kuznetsov, Finite difference schemes for multidimensional first order quasi-linear equations in classes of discontinuous functions, Probl. Math. Phys. Vychisl. Math., Moscow, Nauka (1977) 181–194.
[29] J.O. Langseth, A. Teveito, R. Winther, On the convergence of operator splitting applied to conservation laws with source terms, SIAM J. Numer. Anal. 33 (1996) 843–863.
[30] P. Lax, Shock waves and entropy, in: E.H. Zarantonello (Ed.), Contributions to Nonlinear Functional Analysis, Academic Press, New York, 1971, pp. 603–634.
[31] R. Leveque, Numerical Methods for Conservation Laws, Lectures in Mathematics, ETH Zurich, Birkhauser, 1992.
[32] R.J. LeVeque, Balancing source term and and flux gradients in high resolution Godunov methods: The quasi-steady state wave propagation algoriyhm, J. Comput. Phys. 146 (1998) 346–365.
[33] R.J. LeVeque, D.S.Bale, Wave propagation methods for conservation laws with source terms, preprint.
[34] P.L. Lions, B. Perthame, E. Tadmor, A kinetic formulation of multidimensional scalar conservation laws and related equations, J. Am. Math. Soc. 7 (1994) 169–191.
[35] B. Perthame, Uniqueness and error estimates in first order quasilinear conservation laws via the kinetic entropy defect measure, J. Math. P. et Appl. 77 (1998) 1055–1064.

[36] B. Perthame, An introduction to kinetic schemes for gas dynamics. An introduction to recent developments in theory and numerics for conservation laws (Freiburg/Littenweiler, 1997), in: Lect. Notes Comput. Sci. Eng., 5, Springer, Berlin, 1999, pp. 1–27.
[37] B. Perthame, C. Simeoni, A kinetic scheme for the Saint–Venant system with a source term, ENS preprint 01-13, 2001.
[38] R. Sanders, On the convergence of monotone finite difference schemes with variable spatial differencing, Math. Comput. V.40 (161) (1983) 91–106.
[39] P.K. Smolarkiewicz, L.G. Margolin, MPDATA: a finite-difference solver for geophysical flows, J. Comput. Phys. 140 (1998) 459–480.
[40] A. Szepessy, Convergence of streamline diffusion finite element method for conservation law with boundary conditions, RAIRO Model. Math. Anal. Numer. 25 (1991) 749–783.
[41] B. Van Leer, Towards the ultimate conservation difference schemes, II, J. Comput. Phys. (14) (1974) 361–376.
[42] M.E. Vazquez-Cendon, Improved treatement of source terms in upwind schemes for shallow water equations in channels with irregular geometry, J. Comput. Phys. 148 (2) (1999) 497–526.
[43] J.G. Zhou, D.M. Causon, C.G. Mingham, D.M. Ingram, The surface gradient method for the treatment of source terms in the shallow-water equations, J. Comput. Phys. 168 (2001) 1–25.